

MOX-Report No. 30/2018

**Bootstrap-based Inference for Dependence in
Multivariate Functional Data**

Ieva, F.; Palma, F.; Romo, J.

MOX, Dipartimento di Matematica
Politecnico di Milano, Via Bonardi 9 - 20133 Milano (Italy)

mox-dmat@polimi.it

<http://mox.polimi.it>

Bootstrap-based Inference for Dependence in Multivariate Functional Data

Francesca Ieva PhD^{1*} | Francesco Palma MD^{1*} | Juan Romo PhD^{2†}

¹MOX - Modelling and Scientific Computing, Department of Mathematics, Politecnico di Milano, via Bonardi 9, 20133, Milano, Italy

²Department of Statistics, Universidad Carlos III de Madrid, C/ Madrid, 126 - 28903 Getafe (Madrid) Spain

Correspondence

Francesca Ieva PhD, MOX - Modelling and Scientific Computing, Department of Mathematics, Politecnico di Milano, via Bonardi 9, 20133, Milano, Italy
Email: francesca.ieva@polimi.it

Funding information

In this work, we propose a bootstrap based inferential framework for quantifying dependency among families of multivariate curves. We start from the notion of Spearman index and Spearman Matrix to provide pointwise estimates of dependency among families of (multivariate) curves, enabling the analysis of the pattern of dependence among the components of a multivariate functional dataset. Moreover, a suitable inferential framework for the Spearman index and matrix is proposed, making use of a testing procedure based on suitably adjusted confidence intervals for the Spearman index. An additional bootstrap based test for the matrices, enabling the detection of significant differences in the patterns of dependency among components in different families of multivariate curves, is provided. We apply these procedures to a real case study, where two populations of electrocardiographic signals from healthy and unhealthy patients are compared. All the codes are embedded in a suitable R-package, namely `raohd`. The inferential tools presented in this work represent, to the best of our knowledge, the first systematic attempt to investigate dependency in the (multivariate) functional setting.

KEYWORDS

Spearman index, Spearman Matrix, multivariate functional data,

* Equally contributing authors.

1 | INTRODUCTION

Nowadays, the statistical analysis of complex and high dimensional data is experiencing a notable growth for application in different fields of science such as medicine, finance, criminology, quality control, and many others. This leads to rethink the way the classical statistics approaches the analysis of such data, since methodologies commonly implemented until now for both descriptive and inferential purposes are increasingly limited or inefficient. Data dimensionality often leads multivariate analysis to be not feasible and its results not easily interpretable. Functional Data Analysis (FDA) (see [Ramsay and Silverman \(2005\)](#) [Kokoszka and Reimherr \(2017\)](#) [Ferraty and Vieu \(2006\)](#)), among others, for complete tractation) is clearly the main field of research in statistics which tried to overcome this issue. Despite the fact that several multivariate methods are not usually well suited for functional datasets, many multivariate techniques have inspired advances in FDA. For example, to quantify the relationship of dependence between two or more groups of functional data.

The investigation of the dependence among curves is relatively a new issue in statistics. This is mainly due to the late development of (multivariate) functional data analysis with respect to multivariate analysis as well as to the difficulty in summarizing dependence and other indexes in the infinite dimensional context. In fact, in multivariate statistics the covariance matrix represents the variation of each variable with respect to itself and the other component of a multivariate vector. The analogous object in the multivariate functional case, where functions are indexed by time or space, is not straightforwardly easy to compute, to handle and, in the end, to be interpreted. This is because of the dimension of the variance-covariance operators themselves (in the sampling version), and to the missingness of single indexes that are able to summarize their spectral features and information content. In such context, the use of an alternative nonparametric measure of dependence is considered in order to exploit a manageable index of dependence among components of the multivariate functional data. The idea is to provide a measure of dependence for families of (multivariate) curves, as well as a suitable corresponding inferential framework for testing the presence of dependency among components and possible differences among patterns of dependency.

For instance, [Ogpen-Rhein and Strimmer \(2006\)](#) proposed an estimator for the dynamical correlation introduced by [Dubin and Muller \(2005\)](#) for longitudinal data, which provides a measure of similarity between pairs of functional observations. He et al. in [He et al. \(2000\)](#) and [He et al. \(2004\)](#) proposed a natural way of finding the canonical correlation for functions, previously introduced by [Leurgans et al. \(1993\)](#). They found significant difficulties such as the covariance operator not being invertible, since it is a compact operator that is not generally invertible in infinite dimensional Hilbert space. [Li and Chow \(2005\)](#) provided a generalization of the Pearson correlation coefficient for functional data that allows to quantify the dependence among two families of curves. This measure is called the concordance correlation coefficient and was used to evaluate the reproducibility of repeated-paired curve data. [Valencia et al. \(2012\)](#) defined Kendall's tau coefficient for functions considering pre-orders that permit the sorting of the functional observations and the identification of the concordant and discordant pairs in a bivariate sample of curves. [Ramsay and Silverman \(2005\)](#) also considered a dependence functional measure called the cross-correlation function. This measure provides a surface that evaluates point by point the usual Pearson correlation coefficient between the corresponding values of the pair of curves in two given points.

In this work, we will consider the definition of the Spearman index for function introduced by [Valencia et al. \(2016\)](#) to set a proper inferential framework for assessing dependency among families of (multivariate) curves. The paper is organized as follows: Section 2 recalls some basic notions about depths and the definition of the Spearman index ([S2.1](#))

and Spearman Matrix (§2.2); Section 3 presents the whole inferential framework we propose for assessing the presence of dependency in both univariate and h -variate ($h \geq 2$) functional data. In this part, suitable adjusted bootstrap-based confidence intervals (§3.2) and tests (§3.3) are computed to evaluate the dependency among two families of curves. The framework is extended also to the multivariate case (§3.4). Finally, a bootstrap based test (§3.5) for comparing matrices is used to assess differences in patterns of dependency of two families of multivariate functional data. The effectiveness and reliability of such instruments are proved in a set of simulation studies carried out and detailed in Appendix B. A real case study considering two populations of multivariate Electrocardiographic signals from healthy and unhealthy patients is presented in Section 4. Results are discussed in Section 5, together with possible further developments.

All the analyses are carried out using R Team (2017). Codes are embedded in the `roahd` package, detailed in Tarabelloni et al. (2018).

2 | NONPARAMETRIC ESTIMATION OF DEPENDENCY AMONG (MULTIVARIATE) CURVES

Dependence is the relationship that exists between two or more random variables. The measures of such dependence provide a value that summarizes the size of the association between two variables, which may occur in different ways: (i) the values of one variable increase and the same happens for the other one (*positive association*); (ii) the values of one variable increase and the values of the other one decreases (*negative association*); (iii) there is not consistent behavior of one variable with respect to the other (*uncorrelation/independence*).

To determine the significance of the value given by some association measure, tests of significance are provided for many of them. Such tests hypothesize that there is no relationship between the two variables (i.e., the measure of association is equal to 0). If the measure is far enough from 0, the test shows that there is a significant relationship between the two variables. When there are quantitative variables, what is usually done to interpret dependence is to determine a coefficient of correlation between variables. The decision of what coefficient to use depends on several factors, such as the type of measurement scale in which each variable is expressed, the nature of the distribution and if the dependence sought is linear or nonlinear (see Valencia (2014) for a deeper discussion on this topic). The Pearson coefficient can be used whether the random variables are continuous or discrete, and whether they are measured in intervals or ratios. Although the Pearson coefficient is widely employed, especially in clinical literature, it is not completely satisfactory to measure the dependence between random variables, as it provides limited information about their dependence structure overall in presence of non-linear dependence. The Spearman and Kendall's tau coefficients (Spearman (1904), Xu et al. (2010), Hauke and Kossowski (2011)) are then used, sorting data according to their rank. Also for this reason, they are able to measure dependence when a nonlinear structure exists between the random variables.

Last but not least, the absence of correlation is equivalent to independence in very rare cases, such as when the random variables are Gaussian distributed. Since in the functional case the Normality of the generating process is rare and very difficult to assess at general level, the aim of this part is to introduce inferential instruments for pointwise and interval estimate of dependence among univariate and multivariate functional data.

2.1 | The Spearman index for two families of curves

The Spearman index Spearman (1904) is a non-parametric measure of association between two random variables X and Y . It is defined as the Pearson correlation coefficient between the grades of X and Y and does not require any assumption on the distribution of the variables. One of the possible definition is the following. Let us consider

$(X_1; Y_1)$, $(X_2; Y_2)$ and $(X_3; Y_3)$ as three independent copies of the random vector $(X; Y)$ with joint cumulative distribution function F_{XY} and marginals F_X and F_Y , respectively. The Spearman index between the variables X and Y , denoted by $\rho_s(X, Y)$, is defined as:

$$\rho_s(X, Y) = 3[P\{(X_1 - X_2)(Y_1 - Y_3) > 0\} - P\{(X_1 - X_2)(Y_1 - Y_3) < 0\}] \quad (2.1)$$

The Spearman index is proportional to the difference between the probability of concordance and the probability of discordance for two vectors (X_1, Y_1) and (X_2, Y_3) . However, we are interested in the equivalent definition of ρ_s by computing the Pearson correlation coefficient, indicated with ρ_p , between the random variables $U = F_X(X)$ and $V = F_Y(Y)$, that is:

$$\rho_s(X, Y) = \rho_p(U, V) = \frac{\mathbb{E}(UV) - \mathbb{E}(U)\mathbb{E}(V)}{\sqrt{\text{Var}(U)}\sqrt{\text{Var}(V)}} \quad (2.2)$$

U and V are called the *grades* of X and Y . For this reason, the Spearman index is also called the grade correlation coefficient. Realizations u of U and v of V can be obtained evaluating realizations x of X and y of Y in the distribution functions F_X and F_Y , respectively.

Suppose now to have two samples of size n from the random variables X and Y , say $\mathbf{x} = (x_1, x_2, \dots, x_n)$, $\mathbf{y} = (y_1, y_2, \dots, y_n)$. Consider the vectors of the estimated grades $\mathbf{u} = (u_1, u_2, \dots, u_n)$, $\mathbf{v} = (v_1, v_2, \dots, v_n)$, defined evaluating each observation in the empirical cumulative distribution function of the corresponding sample. So, we have

$$u_i = \hat{F}_X(x_i) = \frac{1}{n} \sum_{j=1}^n \mathbb{I}(x_j \leq x_i) \quad (2.3)$$

$$v_i = \hat{F}_Y(y_i) = \frac{1}{n} \sum_{j=1}^n \mathbb{I}(y_j \leq y_i) \quad (2.4)$$

for $i = 1, \dots, n$. Notice that u_i (resp. v_i) can be interpreted as the relative position of the observation x_i (resp. y_i) in the set \mathbf{x} (resp. \mathbf{y}).

The sample version of the Spearman index is defined as the sample Pearson correlation coefficient of \mathbf{u} and \mathbf{v} :

$$\hat{\rho}_s(\mathbf{x}, \mathbf{y}) = \hat{\rho}_p(\mathbf{u}, \mathbf{v}) = \frac{\sum_{i=1}^n (u_i - \bar{u})(v_i - \bar{v})}{(\sum_{i=1}^n (u_i - \bar{u})^2 \sum_{i=1}^n (v_i - \bar{v})^2)^{1/2}} \quad (2.5)$$

where \bar{u} and \bar{v} stand for the sample means of \mathbf{u} and \mathbf{v} , respectively. Observe that the estimated grades assume always values in $[0, 1]$ and they are bounded independently of the support of the random variables that generated the data. Therefore, an estimate of the Spearman index is less sensitive to the presence of outliers than an estimate of the Pearson correlation coefficient. Finally, we emphasize that ρ_s is well defined for all pairs of random variables. This represents an advantage over the classical Pearson coefficient, which is computable only for pairs of random variables with finite second moment.

The Spearman index satisfies some general and intuitive properties required for any reasonable dependence measure. For instance:

- The sign of ρ_s indicates the direction of association between X and Y . This means that if Y increases when X increases, then the Spearman index is positive (conversely, it is negative if Y increases when X decreases).

- A Spearman index with value 0 indicates that there is not a clear tendency for Y to either increase or decrease when X increases. Moreover, the Spearman index assumes the value 0 when the two random variables are independent.
- The absolute value of ρ_s increases in magnitude as X and Y become closer to being perfect monotone functions of each other. In particular, when X is a monotone increasing function of Y , the index assumes value 1 (−1 if the relation is given by a monotone decreasing function).

These properties show how the Spearman index is able to capture the dependence, either positive or negative, between two random variables, even if the relation is not linear.

This notion has been generalized to the infinite dimensional setting in [Valencia et al. \(2016\)](#), and can be used to assess the presence of dependency between two sets of functions. In order to define the Spearman index for the functional case, some notions enabling the ranking of infinite dimensional objects are needed and recalled below.

Let $C(I)$ be the space of the continuous functions defined in a compact interval I and consider a stochastic process X_t , with distribution L and with sample paths in $C(I)$. The graph of a function x belonging to $C(I)$ is the subset of the plane $G(x) = \{(t, x(t)), t \in I\}$. The hypograph (*hyp*) and the epigraph (*epi*) of x (see [Martin-Barragan et al. \(2016\)](#) for further details) are given respectively by

$$\text{hyp}(x) = \{(t, y) \in I \times \mathbb{R} : y \leq x(t)\}, \quad (2.6)$$

$$\text{epi}(x) = \{(t, y) \in I \times \mathbb{R} : y \geq x(t)\} \quad (2.7)$$

A natural form of ordering curves is considering a curve x as “greater” than another curve y if and only if $\text{hyp}(y) \subset \text{hyp}(x)$ or $\text{epi}(x) \subset \text{epi}(y)$. However, in practical situations the curves in a sample can be crossed and hence the natural ordering in these cases does not work. Therefore, an alternative way of ordering curves can be developed on the basis of two concepts, the *Inferior Length* and the *Superior Length* [Martin-Barragan et al. \(2016\)](#) of a curve with respect to a stochastic process X_t :

$$IL(x) = \frac{1}{\lambda(I)} \mathbb{E}[\lambda\{t \in I : x(t) \geq X_t\}], \quad (2.8)$$

$$SL(x) = \frac{1}{\lambda(I)} \mathbb{E}[\lambda\{t \in I : x(t) \leq X_t\}] \quad (2.9)$$

where λ stands for the Lebesgue measure on \mathbb{R} . Basically the Inferior Length $IL(x)$ is the “proportion of time” that the stochastic process X_t is smaller than x and the Superior Length $SL(x)$ is the “proportion of time” that the stochastic process X_t is greater than x .

These notions are behind the definitions of the *grades* of a stochastic process X_t with respect to another process Z_t :

Definition 1 Let X_t and Z_t be two stochastic processes. Then,

$$IL\text{-grade}(X_t)_{Z_t} = \frac{1}{\lambda(I)} \mathbb{E}_{Z_t}[\lambda\{t \in I : X_t \geq Z_t\}], \quad (2.10)$$

$$SL\text{-grade}(X_t)_{Z_t} = \frac{1}{\lambda(I)} \mathbb{E}_{Z_t}[\lambda\{t \in I : X_t \leq Z_t\}]. \quad (2.11)$$

Observe that *IL-grade* and *SL-grade* assign a value between $[0, 1]$ to X_t . To avoid hard notation, the subscript Z_t is neglected when the two processes have the same distribution.

Consider now a functional dataset $x_1(t), \dots, x_n(t)$, with $t \in I$, composed by n realizations of the process X_t . If we fix any curve $x = x(t)$ of the dataset, the sample version of both *IL-grade* and *SL-grade* can be easily obtained by substituting the expectation with the sample mean as follows:

$$IL_n\text{-grade}(x) = \frac{1}{n\lambda(I)} \sum_{j=1}^n \lambda\{t \in I : x(t) \geq x_j(t)\}, \quad (2.12)$$

$$SL_n\text{-grade}(x) = \frac{1}{n\lambda(I)} \sum_{j=1}^n \lambda\{t \in I : x(t) \leq x_j(t)\}. \quad (2.13)$$

$IL_n\text{-grade}(x)$ and $SL_n\text{-grade}(x)$ quantify the relative position of x with respect to the other curves of the sample. From (2.13), it can be noticed that the largest grade in a functional dataset may not be 1 unless the curve with the highest grade does not cross with any other.

The sample version of the Inferior and Superior Length grade provide an affective way for ordering a set of curves. In fact, we can give the following criterion:

Definition 2 Consider the functional dataset $x_1(t), \dots, x_n(t)$, with $t \in I$, composed by n realizations of a stochastic process X_t . Then,

$$x_i(t) \leq x_j(t) \Leftrightarrow IL_n\text{-grade}(x_i) \leq IL_n\text{-grade}(x_j).$$

The alternative definition can be deduced by replacing the IL_n -grade with SL_n -grade.

The relation given by Definition 2 meets important properties such as reflectivity and transitivity, but, unfortunately, it does not satisfy the antisymmetry property. Therefore, the relation introduced is a pre-order, which is less restrictive than a partial order and allows to compare any pair of functions in the sample.

Given the previous framework, the Spearman index for two stochastic processes can be introduced as follows:

Definition 3 (Spearman index for stochastic processes) Let (X_t, Y_t) be a stochastic process with law L taking values on the space $C(I; \mathbb{R}^2)$ of the continuous functions $(f(t), g(t)) : I \rightarrow \mathbb{R}^2$, with I a compact interval of \mathbb{R} . The Spearman index for (X_t, Y_t) is defined as

$$\rho_s(X_t, Y_t) = \rho_p(IL\text{-grade}(X_t), IL\text{-grade}(Y_t)), \quad (2.14)$$

where ρ_p denotes the Pearson correlation coefficient and $IL\text{-grade}(\cdot)$ is the grade associated to a stochastic process, as in Definition 1.

The corresponding sample version is the following:

Definition 4 (Sample Spearman index for bivariate functional dataset) Consider the bivariate functional dataset,

$$\begin{bmatrix} \mathbf{x} & \mathbf{y} \end{bmatrix} = \begin{bmatrix} x_1(t) & y_1(t) \\ x_2(t) & y_2(t) \\ \vdots & \vdots \\ x_n(t) & y_n(t) \end{bmatrix}_{t \in I},$$

composed by n realizations of the stochastic process (X_t, Y_t) as above. Then, the sample Spearman index, denoted by $\hat{\rho}_s(\mathbf{x}, \mathbf{y})$, is defined as

$$\hat{\rho}_s(\mathbf{x}, \mathbf{y}) = \hat{\rho}_p(IL_n - grade(\mathbf{x}), IL_n - grade(\mathbf{y})), \quad (2.15)$$

where $\hat{\rho}_p$ is the sample Pearson correlation coefficient and

$$\begin{aligned} IL_n - grade(\mathbf{x}) &= (IL_n - grade(x_1), IL_n - grade(x_2), \dots, IL_n - grade(x_n)), \\ IL_n - grade(\mathbf{y}) &= (IL_n - grade(y_1), IL_n - grade(y_2), \dots, IL_n - grade(y_n)). \end{aligned} \quad (2.16)$$

An alternative definition of the Spearman index for functions can be obtained by replacing IL_n -grade by SL_n -grade.

The Spearman index defined above satisfies (see [Valencia et al. \(2016\)](#) for proofs) some desirable properties required for a dependence measure (see [Xu et al. \(2010\)](#)), in particular:

- ρ_s is well defined for any (X_t, Y_t) .
- $\rho_s(X_t, Y_t) = \rho_s(Y_t, X_t)$.
- $-1 \leq \rho_s(X_t, Y_t) \leq 1$.
- $\rho_s(X_t, g(X_t)) = 1$ for any increasing function g .
- $\rho_s(X_t, g(X_t)) = -1$ for any decreasing function g .
- The Spearman index is invariant under strictly increasing transformations of the processes, that is:

$$\rho_s(\alpha(X_t), \beta(Y_t)) = \rho_s(X_t, Y_t), \quad (2.17)$$

for any $\alpha(\cdot)$ and $\beta(\cdot)$ being strictly increasing functions.

- If X_t and Y_t are stochastically independent, then $\rho_s(X_t, Y_t) = 0$.
- The sample Spearman index is a consistent estimator of the index of the original processes.

The Spearman index can then be used for assessing dependency among two stochastic processes (i.e., two families of univariate functional data). The same is true also in the case these two processes are the components of a bivariate functional data, i.e., a bivariate stochastic process where each statistical unit is characterized by a bivariate function $(X_1(t), X_2(t))$. The latter view of the problem naturally leads to the generalization of the inferential paradigm to the h -variate case.

2.2 | Spearman Matrix for h -variate functional data

Up to now, we only considered bivariate functional data. Nevertheless, in real problems it is more and more often the case that a statistical unit is described through a set of h curves, with $h \in \mathbb{N}$ and, possibly, $h > 2$. This is particularly true for biological problems, where vital signs often are measured for monitoring the health status of a patient. Therefore, in such a framework investigating the way the components of multivariate functional data depend one on each other is a challenging and fascinating problem. In multivariate statistics, the covariance matrix represents the variation of each variable with respect to itself and the other component of a multivariate vector. The analogous object in the multivariate functional case, i.e., the variance-covariance operator, is not straightforwardly easy to compute, to handle and, in the end, to be interpreted and used for the same purpose. This is firstly due to its dimension once dealing with the corresponding sampling version, and to the missingness of single indexes that are able to summarize its spectral features and information content.

These reasons led us to introduce a new mathematical object, based on the nonparametric index described in the previous Section, for expressing in an intuitive way the pattern of dependence among the components of multivariate functional data.

Let $\mathbf{X}_t = (X_t^1, X_t^2, \dots, X_t^h)$ be a stochastic process with law L taking values on the space $C(I; \mathbb{R}^h)$ of the vector-valued continuous functions $f(t) : I \rightarrow \mathbb{R}^h$, with I a compact interval of \mathbb{R} and $h > 2$. We define the *Spearman Matrix* (SM in the following) as the $h \times h$ symmetric matrix

$$SM(\mathbf{X}_t) = \begin{bmatrix} \rho_s(X_t^1, X_t^1) & \rho_s(X_t^1, X_t^2) & \dots & \rho_s(X_t^1, X_t^h) \\ \rho_s(X_t^2, X_t^1) & \rho_s(X_t^2, X_t^2) & \dots & \rho_s(X_t^2, X_t^h) \\ \vdots & \vdots & \ddots & \vdots \\ \rho_s(X_t^h, X_t^1) & \rho_s(X_t^h, X_t^2) & \dots & \rho_s(X_t^h, X_t^h) \end{bmatrix}, \quad (2.18)$$

where $\rho_s(X_t^i, X_t^j)$ is the Spearman index between the i -th and j -th component of the stochastic process, as in Definition 3. Let then

$$\mathbf{X} = \begin{bmatrix} \mathbf{x}_1 & \mathbf{x}_2 & \dots & \mathbf{x}_h \end{bmatrix} = \begin{bmatrix} x_{1,1}(t) & x_{1,2}(t) & \dots & x_{1,h}(t) \\ x_{2,1}(t) & x_{2,2}(t) & \dots & x_{2,h}(t) \\ \dots & \dots & \dots & \dots \\ x_{n,1}(t) & x_{n,2}(t) & \dots & x_{n,h}(t) \end{bmatrix}_{t \in I}, \quad (2.19)$$

be a multivariate functional dataset, composed by n realizations of the stochastic process \mathbf{X}_t , where the vectors

$$\mathbf{x}_i = (x_{1,i}(t), x_{2,i}(t), \dots, x_{n,i}(t))'_{t \in I}, \quad i = 1, \dots, h \quad (2.20)$$

represent the functional samples containing the realizations of a specific component of the process. To avoid hard notations, the vectors are represented neglecting the dependence on time. The sample Spearman Matrix $\widehat{SM}(\mathbf{X})$ is given by

$$\widehat{SM}(\mathbf{X}) = \begin{bmatrix} \hat{\rho}_s(\mathbf{x}_1, \mathbf{x}_1) & \hat{\rho}_s(\mathbf{x}_1, \mathbf{x}_2) & \dots & \hat{\rho}_s(\mathbf{x}_1, \mathbf{x}_h) \\ \hat{\rho}_s(\mathbf{x}_2, \mathbf{x}_1) & \hat{\rho}_s(\mathbf{x}_2, \mathbf{x}_2) & \dots & \hat{\rho}_s(\mathbf{x}_2, \mathbf{x}_h) \\ \vdots & \vdots & \ddots & \vdots \\ \hat{\rho}_s(\mathbf{x}_h, \mathbf{x}_1) & \hat{\rho}_s(\mathbf{x}_h, \mathbf{x}_2) & \dots & \hat{\rho}_s(\mathbf{x}_h, \mathbf{x}_h) \end{bmatrix}, \quad (2.21)$$

where $\hat{\rho}_s(\mathbf{x}_i, \mathbf{x}_j)$ is the sample Spearman index computed on the bivariate functional dataset $[\mathbf{x}_i \ \mathbf{y}_j]$, as in Definition 4. It can be immediately noticed that $\widehat{SM}(\mathbf{X})$ is an easy to handle and easy to interpret mathematical object and its cross diagonal elements give a quick and effective overview of the pattern of dependence among components of a multivariate functional dataset.

Since $SM(\mathbf{X}_t)$ and $\widehat{SM}(\mathbf{X})$ are symmetric, in the following we will show only their upper triangular part.

3 | A BOOTSTRAP-BASED INFERENCE FRAMEWORK FOR SPEARMAN INDEX AND MATRIX

In this Section, we aim at defining an inferential framework for the Spearman index and Matrix making use of the bootstrap methodology. Bootstrap is a computationally intensive technique for assigning measures of accuracy to statistical estimates in a non-parametric framework. This approach has a wide range of applications (see [Efron and Tibshirani \(1993\)](#) for more details) and it can be also exploited, in an inferential perspective, to implement test and compute confidence intervals for any parameter of interest.

The purpose we use the bootstrap methodology for is twofold: firstly, we aim at defining suitable confidence intervals for the Spearman index estimates, in order to assess if the Spearman index computed among two families of curves is significantly different from 0. Notice that this step represents an improvement of [Valencia et al. \(2016\)](#), where only the point estimate of the index is provided. Suitable applications of this bootstrap methodology enable us to define properly hypothesis tests for checking the independence of two families of functional data. Moreover, the bootstrap methods are also used for defining a procedure testing the possible difference among two matrices (Section 3.5).

3.1 | Preliminary notions on bootstrap techniques applied to the distribution of Spearman index

Let (X_1, \dots, X_n) be independent and identically distributed random variables with probability distribution F and suppose that a sample $\mathbf{x} = (x_1, \dots, x_n)$ is available. Let's assume that the inferential purpose is to estimate a parameter of interest $\theta = t(F)$, on the basis of \mathbf{x} and for this purpose we consider the estimator T_n , whose value in the sample is $\hat{\theta} = T_n(\mathbf{x})$. The sampling distribution of the statistic T_n , that we call G and that we supposed unknown in this framework, is completely determined by F and n . We aim at defining a method to estimate G . A possible approach can be the following. Consider $\mathbf{x}_1, \mathbf{x}_2, \dots, \mathbf{x}_B$, being B samples of size n drawn from F , say

$$\mathbf{x}_i = (x_{i,1}, x_{i,2}, \dots, x_{i,n}), \quad x_{i,1}, \dots, x_{i,n} \sim F \quad i.i.d., \quad i = 1, \dots, B,$$

and compute $\hat{\theta}(i) = T_n(\mathbf{x}_i), i = 1, \dots, B$. In this way, we obtain the replications

$$\hat{\theta}(1), \hat{\theta}(2), \dots, \hat{\theta}(B),$$

that are distributed according to G . We can use the informations provided by the replications to approximate the shape of the sampling distribution G as well as to evaluate the accuracy of the estimate $\hat{\theta} = T_n(\mathbf{x})$. This latter operation is possible computing, for instance, an estimate of $\hat{\theta}$ standard error (i.e., an estimate of the standard deviation of the distribution G). Therefore, using this approach, we have the possibility to study the properties of the statistic of interest simply evaluating its behaviour on samples of size n drawn directly from F .

However, this method cannot be used in practical situations since the distribution F is not known. The bootstrap method uses a different strategy, based on the notion of *bootstrap sample*. Let then \hat{F} be the empirical distribution of F , say a discrete distribution that puts probability $1/n$ on each value $x_i, i = 1, 2, \dots, n$. In other words, the empirical distribution represents an estimate of the underlying model that generated the data \mathbf{x} . A bootstrap sample \mathbf{x}^* is defined to be a random sample of size n drawn from \hat{F} , say

$$\mathbf{x}^* = (x_1^*, x_2^*, \dots, x_n^*), \quad x_1^*, x_2^*, \dots, x_n^* \sim \hat{F} \quad i.i.d. \quad (3.1)$$

The star notation indicates that \mathbf{x}^* is not the actual dataset \mathbf{x} , but rather a randomized, or *resampled*, version of \mathbf{x} . There is another way to write down (3.1). The bootstrap data points $x_1^*, x_2^*, \dots, x_n^*$ are a random sample of size n drawn with replacement from the population of n equally likely objects (x_1, x_2, \dots, x_n) .

The bootstrap method uses the same approach described above simply substituting F with its empirical version \hat{F} . Consider $\mathbf{x}_1^*, \mathbf{x}_2^*, \dots, \mathbf{x}_B^*, B$ bootstrap samples from \hat{F} , namely

$$\mathbf{x}_i^* = (x_{i,1}^*, x_{i,2}^*, \dots, x_{i,n}^*), \quad x_{i,1}^*, \dots, x_{i,n}^* \sim \hat{F} \quad i.i.d., \quad i = 1, \dots, B, \quad (3.2)$$

and compute $\hat{\theta}^*(i) = T_n(\mathbf{x}_i^*), i = 1, \dots, B$. In so doing, we obtain the collection of bootstrap replications

$$\hat{\theta}^*(1), \hat{\theta}^*(2), \dots, \hat{\theta}^*(B), \quad (3.3)$$

that represents a sample from the so called *bootstrap distribution* of the statistic T_n . Therefore, the bootstrap distribution of a statistic is its distribution when data used to evaluate it are bootstrap samples obtained, with suitable resamplings, from the original dataset. Of course, the bootstrap distribution is not unique, since it depends on the observations used to define \hat{F} . Theoretically, a statistic has infinite bootstrap distributions, one for each possible sample \mathbf{x} of size n drawn from F .

Let's now suppose to obtain a sample from the bootstrap distribution of the statistic $\hat{\rho}_s(\mathbf{x}, \mathbf{y})$ of interest. Consider the functional dataset from the stochastic process (X_t, Y_t) ,

$$\begin{bmatrix} \mathbf{x} & \mathbf{y} \end{bmatrix} = \begin{bmatrix} x_1(t) & y_1(t) \\ x_2(t) & y_2(t) \\ \vdots & \vdots \\ x_n(t) & y_n(t) \end{bmatrix}_{t \in T}, \quad (3.4)$$

composed by n bivariate curves observed on the time grid $T = \{t_1, t_2, \dots, t_d\}$. The bootstrap resampling requires an empirical estimate of the stochastic model F that generated the data. The stochastic model F is then estimated with its empirical version \hat{F} , namely with a discrete distribution that assigns probability $1/n$ to each of the n bivariate curves of the dataset. We define the bootstrap sample $[\mathbf{x}^* \quad \mathbf{y}^*]$ as a random sample of size n drawn from \hat{F} , i.e., n bivariate curves drawn with replacement and with uniform probability from the population defined by (3.4). An equivalent representation is the following:

$$[\mathbf{x}^* \quad \mathbf{y}^*] = \begin{bmatrix} x_{\pi_1}(t) & y_{\pi_1}(t) \\ x_{\pi_2}(t) & y_{\pi_2}(t) \\ \vdots & \vdots \\ x_{\pi_n}(t) & y_{\pi_n}(t) \end{bmatrix}_{t \in T} \quad (3.5)$$

where $(\pi_1, \pi_2, \dots, \pi_n)$ is a random sample from the uniform distribution on the discrete set $\{1, 2, \dots, n\}$.

Fixed this notion, we can now compute the bootstrap replications of the statistic $\hat{\rho}_s(\mathbf{x}, \mathbf{y})$ as reported in Table 3. The procedure generates the collection

$$\hat{\rho}^*(1), \hat{\rho}^*(2), \dots, \hat{\rho}^*(B), \quad (3.6)$$

that may be used to approximate the shape of the distribution of $\hat{\rho}_s(\mathbf{x}, \mathbf{y})$. Given these notions, we are now ready to present bootstrap-based methods to compute confidence intervals.

3.2 | Bootstrap confidence intervals for the Spearman Index ρ_s

In this Section we aim at providing a confidence interval for the Spearman index ρ_s in order to set the first part of the inferential framework to be used in investigations of dependence of multivariate functional data. The second part will be given in the next Section, where a suitable hypothesis test for dependency is presented.

Appendix A reports general theoretical notions on the construction of bootstrap based confidence intervals. In our case, it translates into the idea of constructing an interval estimate for ρ_s using the informations provided by the bootstrap distribution of the estimator $\hat{\rho}_s$. We decide to use the BC_a intervals (see Appendix A) since they represent, in terms of efficiency and accuracy, the best choice in the literature of the bootstrap methods (see Efron (1987) for a detailed discussion on this).

Definition 5 (Confidence interval for the Spearman index) Consider the functional dataset from the stochastic process (X_t, Y_t) ,

$$[\mathbf{x} \quad \mathbf{y}] = \begin{bmatrix} x_1(t) & y_1(t) \\ x_2(t) & y_2(t) \\ \vdots & \vdots \\ x_n(t) & y_n(t) \end{bmatrix}_{t \in T},$$

TABLE 1 Pseudo-code of the bootstrap procedure used to compute the bootstrap distribution of $\hat{\rho}(x, y)$ **Algorithm 1:** Bootstrap distribution of the Spearman coefficient $\hat{\rho}_s(x, y)$.**Input:** Functional dataset

$$\begin{bmatrix} \mathbf{x} & \mathbf{y} \end{bmatrix} = \begin{bmatrix} x_1(t) & y_1(t) \\ x_2(t) & y_2(t) \\ \vdots & \vdots \\ x_n(t) & y_n(t) \end{bmatrix}_{t \in T}$$

1 **for** $i \in 1, \dots, B$ **do**2 obtain $\pi_1^i, \pi_2^i, \dots, \pi_n^i$ from the uniform distribution on the discrete set $\{1, 2, \dots, n\}$;3 define the **BOOTSTRAP SAMPLE**

$$\begin{bmatrix} \mathbf{x}_i^* & \mathbf{y}_i^* \end{bmatrix} = \begin{bmatrix} x_{\pi_1^i}(t) & y_{\pi_1^i}(t) \\ x_{\pi_2^i}(t) & y_{\pi_2^i}(t) \\ \vdots & \vdots \\ x_{\pi_n^i}(t) & y_{\pi_n^i}(t) \end{bmatrix}_{t \in T}$$

 compute the **BOOTSTRAP REPLICATION** $\hat{\rho}^*(i) = \hat{\rho}_s(\mathbf{x}_i^*, \mathbf{y}_i^*)$.

composed by n bivariate curves observed on the time grid $T = \{t_1, t_2, \dots, t_d\}$. Let

$$\hat{\rho}^*(1), \hat{\rho}^*(2), \dots, \hat{\rho}^*(B)$$

be B bootstrap replications of the estimator $\hat{\rho}_s$. The BC_a confidence interval for $\rho_s(X_t, Y_t)$ of coverage probability of $1 - \alpha$ is given by

$$CI_{1-\alpha}(\rho_s) = (\hat{\rho}_B^{*(\alpha_1)}, \hat{\rho}_B^{*(\alpha_2)}), \quad (3.7)$$

where $\hat{\rho}_B^{*(\alpha_1)}$ and $\hat{\rho}_B^{*(\alpha_2)}$ are respectively the $100 \cdot \alpha_1$ th and the $100 \cdot \alpha_2$ th empirical percentiles of the bootstrap replications.

The order α_1 and α_2 of the percentiles are obtained according to the procedure described in Appendix A. Table 7 summarizes the entire procedure which enables the construction of confidence intervals for the Spearman coefficient among two stochastic processes.

3.3 | An independence bootstrap based test for bivariate functional data

Another useful inferential tool we introduce is a bootstrap-based test aimed at checking if the Spearman index between two families of functional data can be considered as equal to zero or not. Since a null value of the index expresses a

condition of independence, this tool allows for verifying whether two families of curves are uncorrelated.

Let then (X_t, Y_t) be a stochastic process with law L taking values on the space $C(I; \mathbb{R}^2)$ of the continuous functions $(f(t), g(t)) : I \rightarrow \mathbb{R}^2$, with I a compact interval of \mathbb{R} . Suppose to have the functional dataset

$$\begin{bmatrix} \mathbf{x} & \mathbf{y} \end{bmatrix} = \begin{bmatrix} x_1(t) & y_1(t) \\ x_2(t) & y_2(t) \\ \vdots & \vdots \\ x_n(t) & y_n(t) \end{bmatrix}_{t \in T},$$

composed by n bivariate curves observed on the time grid $T = \{t_1, t_2, \dots, t_d\}$, realizations of (X_t, Y_t) . We want to check the following hypotheses:

$$H_0 : \rho_s(X_t, Y_t) = 0,$$

$$H_1 : \rho_s(X_t, Y_t) \neq 0.$$

In other words, the test aims at providing evidence for a possible dependency among two families of functional data. It can be carried out in more than one way: a possible implementation is the one proposed in [Valencia et al. \(2016\)](#). In order to maintain the coherence with the previous framework, we propose here the following criterion:

Reject H_0 if the Bias-corrected and accelerated confidence interval for the Spearman index $BC_a(\rho_s)$ of intended coverage probability $1 - \alpha$ does not contain zero.

Using this approach, we essentially exploit the BC_a intervals for the Spearman index introduced in 3.2 within a test procedure framework. The simulation studies reported in Appendix B show the effectiveness of our approach.

3.4 | Inference for h-variate functional data

The concepts presented in Sections 3.2 and 3.3 for couples of stochastic processes are useful and straightforward to be translated into the case of multivariate functional data. In fact, considering the case where the observations are realizations of the stochastic process $\mathbf{X}_t = (X_t^1, X_t^2, \dots, X_t^h)$, with $h > 2$, the pattern of dependence between the components is captured by the Spearman Matrix $SM(\mathbf{X}_t)$ presented in Section 2.2, whose entry ij represents the Spearman index between the i th and j th component of the multivariate functional data, say $\rho_s(X_t^i, X_t^j)$.

In fact, given the procedure to derive a confidence interval for the Spearman index, we can exploit it to define interval estimates for each component of the dependency pattern resumed by the Spearman matrix. Therefore, we define the $h \times h$ symmetric matrix

$$\widehat{SM}(\mathbf{X})_{1-\alpha} = \begin{bmatrix} 1 & CI_{1-\alpha}^{1,2} & \dots & \dots & CI_{1-\alpha}^{1,h} \\ & 1 & CI_{1-\alpha}^{2,3} & \dots & CI_{1-\alpha}^{2,h} \\ & & 1 & \vdots & \vdots \\ & & & 1 & CI_{1-\alpha}^{h-1,h} \\ & & & & 1 \end{bmatrix}, \quad (3.8)$$

where $CI_{1-\alpha}^{i,j}$, $i = 1, \dots, h-1, j = i+1, \dots, h$ stands for the BC_a interval of coverage probability $1 - \alpha$ for $\rho_s(X_t^i, X_t^j)$.

The same is true for the testing procedure described in 3.3. In this case, we can perform the pairwise disjoint tests

$$\begin{aligned} H_0 &: \rho_s(X_t^i, X_t^j) = 0, \\ H_1 &: \rho_s(X_t^i, X_t^j) \neq 0. \end{aligned}$$

for $i = 1, \dots, h-1, j = i+1, \dots, h$. In doing so, we do detect the components that are significantly different from 0 in the pattern of dependency. Therefore, flanking the pointwise estimate of the Spearman Matrix

$$\widehat{SM}(\mathbf{X}) = \begin{bmatrix} \hat{\rho}_s(\mathbf{x}^1, \mathbf{x}^1) & \hat{\rho}_s(\mathbf{x}^1, \mathbf{x}^2) & \dots & \hat{\rho}_s(\mathbf{x}^1, \mathbf{x}^h) \\ \hat{\rho}_s(\mathbf{x}^2, \mathbf{x}^1) & \hat{\rho}_s(\mathbf{x}^2, \mathbf{x}^2) & \dots & \hat{\rho}_s(\mathbf{x}^2, \mathbf{x}^h) \\ \vdots & \vdots & \ddots & \vdots \\ \hat{\rho}_s(\mathbf{x}^h, \mathbf{x}^1) & \hat{\rho}_s(\mathbf{x}^h, \mathbf{x}^2) & \dots & \hat{\rho}_s(\mathbf{x}^h, \mathbf{x}^h) \end{bmatrix}, \quad (3.9)$$

with the matrix of confidence intervals

$$\widehat{SM}(\mathbf{X})_{1-\alpha} = \begin{bmatrix} 1 & CI_{1-\alpha}^{1,2} & \dots & \dots & CI_{1-\alpha}^{1,h} \\ & 1 & CI_{1-\alpha}^{2,3} & \dots & CI_{1-\alpha}^{2,h} \\ & & 1 & \vdots & \vdots \\ & & & 1 & CI_{1-\alpha}^{h-1,h} \\ & & & & 1 \end{bmatrix}, \quad (3.10)$$

we provide an useful and manageable tool for the detection of significant dependency among components of multivariate functional data. In fact, if the confidence interval for $\rho_s(X_t^i, X_t^j)$ contains zero, there is no evidence (with respect to a significance level α) to assume a dependence between the i th and j th component of the multivariate curves. The corresponding entry ij of $\widehat{SM}(\mathbf{X})$ may be considered as equal to zero. To simplify the pattern, only significant components may be highlighted.

3.5 | Bootstrap test for the equality of two Spearman Matrices

As it is the case in multivariate statistics, sometimes the interest of the analysis may lie in the comparison among the patterns of dependency of two or more families of multivariate functional data. For example, if the statistical units under study are characterized by multivariate signals, we might wonder if people belonging to different groups present the same pattern of dependency among components of their curves or not. This is the case also considered for the real

case study presented in Section 4.

For this reason, we now propose a bootstrap-based test procedure to check the dissimilarity of two Spearman matrices, referring to two populations of multivariate functional data. Suppose $(\mathbf{X}_t, \mathbf{Y}_t)$ to be two h -variate ($h > 2$) stochastic processes of the form

$$\mathbf{X}_t = (X_t^1, X_t^2, \dots, X_t^h), \quad \mathbf{Y}_t = (Y_t^1, Y_t^2, \dots, Y_t^h),$$

and assume that the same continuity assumption of Definition 3 holds for both processes. Assume also to have the multivariate functional datasets

$$\mathbf{X} = \begin{bmatrix} x_{1,1}(t) & x_{1,2}(t) & \dots & x_{1,h}(t) \\ x_{2,1}(t) & x_{2,2}(t) & \dots & x_{2,h}(t) \\ \dots & \dots & \dots & \dots \\ x_{n_x,1}(t) & x_{n_x,2}(t) & \dots & x_{n_x,h}(t) \end{bmatrix}_{t \in \mathcal{T}},$$

$$\mathbf{Y} = \begin{bmatrix} y_{1,1}(t) & y_{1,2}(t) & \dots & y_{1,h}(t) \\ y_{2,1}(t) & y_{2,2}(t) & \dots & y_{2,h}(t) \\ \dots & \dots & \dots & \dots \\ y_{n_y,1}(t) & y_{n_y,2}(t) & \dots & y_{n_y,h}(t) \end{bmatrix}_{t \in \mathcal{T}},$$

from \mathbf{X}_t and \mathbf{Y}_t , respectively. We want to perform the test

$$\begin{aligned} H_0 &: SM(\mathbf{X}_t) = SM(\mathbf{Y}_t), \\ H_1 &: SM(\mathbf{X}_t) \neq SM(\mathbf{Y}_t). \end{aligned}$$

The main issue in checking these hypotheses is the definition of a suitable test statistic that is sensible to departures from H_0 . Here we propose a test statistic based on the notion of distance between two matrices.

Let d a distance in the space $\mathbb{R}^{h \times h}$, say a binary function

$$d(\cdot, \cdot) : \mathbb{R}^{h \times h} \times \mathbb{R}^{h \times h} \rightarrow \mathbb{R}$$

such that, for any $A, B, C \in \mathbb{R}^{h \times h}$:

- $d(A, B) \geq 0$ and $d(A, B) = 0$ if and only if $A = B$;
- $d(A, B) = d(B, A)$;
- $d(A, B) \leq d(A, C) + d(C, B)$.

The notion of distance is suited for defining a statistic that captures deviations from the null hypothesis. In fact, the value returned by d is expression of the dissimilarity of two matrices since it takes in account the differences they

present. With this in mind, we propose to check H_0 exploiting the statistic

$$\Phi(\mathbf{X}, \mathbf{Y}) = d(\widehat{SM}(\mathbf{X}), \widehat{SM}(\mathbf{Y})). \quad (3.11)$$

Our choice is quite reasonable. In fact, large values of Φ denote great distance among the sample Spearman matrices of the two populations of multivariate functional data, providing evidence in favour of the dissimilarity of the Spearman matrices of the generative processes.

Thus, our test procedure requires a notion of distance in the space of the $h \times h$ matrices. We can introduce it considering the distance induced by a matrix norm. In fact, let $\|\cdot\|$ be a norm in the space $\mathbb{R}^{h \times h}$, say an application

$$\|\cdot\| : \mathbb{R}^{h \times h} \rightarrow \mathbb{R}$$

such that, for any $A, B \in \mathbb{R}^{h \times h}$:

- $\|A\| \geq 0$ and $\|A\| = 0$ if and only if $A = 0$;
- $\|\alpha A\| = |\alpha| \|A\| \forall \alpha \in \mathbb{R}$;
- $\|A + B\| \leq \|A\| + \|B\|$.

It can be shown, exploiting the properties of the norm, that the function

$$d(A, B) = \|A - B\|, \quad A, B \in \mathbb{R}^{h \times h},$$

defines a distance in the space $\mathbb{R}^{h \times h}$. Therefore, a matrix norm provides also a notion of distance (and dissimilarity) among matrices. Given $A \in \mathbb{R}^{h \times h}$, some examples of norms are:

- *One norm*: $\|A\|_1 = \max_{j=1, \dots, h} \sum_{i=1}^h |a_{ij}|$;
- *Infinity norm*: $\|A\|_\infty = \max_{i=1, \dots, h} \sum_{j=1}^h |a_{ij}|$;
- *Frobenius norm*: $\|A\|_F = \sqrt{\sum_{i=1}^h \sum_{j=1}^h |a_{ij}|^2}$.

Notice that the three norms assume small values when the entries of the matrix are small, so the corresponding distances show small values when the difference of the two matrices has small entries, i.e., when the two matrices are almost equal. Therefore, the distances induced by them represent an effective way to capture dissimilarity among matrices. Summing up, we propose to test H_0 exploiting the test statistic

$$\Phi(\mathbf{X}, \mathbf{Y}) = \|\widehat{SM}(\mathbf{X}) - \widehat{SM}(\mathbf{Y})\|, \quad (3.12)$$

being $\|\cdot\|$ a suitable norm in the space of the $h \times h$ matrices.

Since the statistic distribution under H_0 is not a priori known, again we propose, coherently with the previous framework of the paper, to approximate it using the bootstrap methodology. The idea is to compute bootstrap replications of Φ under the null hypothesis and to compare them with the observed value $\Phi(\mathbf{X}, \mathbf{Y})$ to estimate the p-value of the test. Table 4 sketches the bootstrap procedure for testing the equality of two Spearman matrices.

Note that the resampling which allows to reproduce the bootstrap datasets $\mathbf{X}_0^*, \mathbf{Y}_0^*$ under the null hypothesis is based on the following argument: under H_0 , the generative processes have the same pattern of dependence among components, so each of the multivariate curves

$$\begin{aligned} (x_{i,1}(t), x_{i,2}(t), \dots, x_{i,h}(t))_{t \in T}, \quad i = 1, \dots, n_x, \\ (y_{i,1}(t), y_{i,2}(t), \dots, y_{i,h}(t))_{t \in T}, \quad i = 1, \dots, n_y, \end{aligned} \quad (3.13)$$

are equally likely in both populations. Therefore, we can consider the set of the $n_x + n_y$ curves given by 3.13 and define a discrete distribution \hat{F}_0 that assigns probability $1/(n_x + n_y)$ to each of them. The bootstrap datasets $\mathbf{X}_0^*, \mathbf{Y}_0^*$ are then defined as two random samples of size n_x and n_y , respectively, drawn from \hat{F}_0 .

With this test we end up with a complete inferential framework to assess dependency of two or more families of (multivariate) curves. Appendix B presents a simulation study aimed at verifying the performances and reliability of the proposed methods in many different scenarios. We remind that all the procedures described are implemented in the R-package `roahd` (see [Tarabelloni et al. \(2018\)](#)).

TABLE 2 Pseudo-code of the bootstrap procedure used to compute the Bias-corrected and accelerated confidence intervals for $\rho(\mathbf{x}, \mathbf{y})$.

Algorithm 2: Bias-corrected and accelerated confidence intervals for the Spearman coefficient $\rho_s(\mathbf{x}, \mathbf{y})$.

Input: Functional dataset

$$\begin{bmatrix} \mathbf{x} & \mathbf{y} \end{bmatrix} = \begin{bmatrix} x_1(t) & y_1(t) \\ x_2(t) & y_2(t) \\ \vdots & \vdots \\ x_n(t) & y_n(t) \end{bmatrix}_{t \in T}$$

1 **for** $i \in 1, \dots, B$ **do**

2 obtain $\pi_1^i, \pi_2^i, \dots, \pi_n^i$ from the uniform distribution on the discrete set $\{1, 2, \dots, n\}$;

3 define the **BOOTSTRAP SAMPLE**

$$\begin{bmatrix} \mathbf{x}_j^* & \mathbf{y}_j^* \end{bmatrix} = \begin{bmatrix} x_{\pi_1^i}(t) & y_{\pi_1^i}(t) \\ x_{\pi_2^i}(t) & y_{\pi_2^i}(t) \\ \vdots & \vdots \\ x_{\pi_n^i}(t) & y_{\pi_n^i}(t) \end{bmatrix}_{t \in T}$$

 compute the **BOOTSTRAP REPLICATION** $\hat{\rho}^*(i) = \hat{\rho}_s(\mathbf{x}_j^*, \mathbf{y}_j^*)$;

4 compute the **JACKKNIFE VALUES** as

$$\hat{\theta}_{(i)} = \hat{\rho}_s(\mathbf{x}_{(i)}, \mathbf{y}_{(i)}), \quad i = 1, \dots, n,$$

where $(\mathbf{x}_{(i)}, \mathbf{y}_{(i)})$ stands for the bivariate functional sample with the i -th bivariate curve removed;

5 compute the **ACCELERATION** as

$$\hat{a} = \frac{\sum_{i=1}^n (\hat{\theta}_{(\cdot)} - \hat{\theta}_{(i)})^3}{6 \{ \sum_{i=1}^n (\hat{\theta}_{(\cdot)} - \hat{\theta}_{(i)})^2 \}^{3/2}}.$$

where $\hat{\theta}_{(\cdot)} = \sum_{i=1}^n \hat{\theta}_{(i)} / n$;

6 compute the **BIAS-CORRECTION** as

$$\hat{z}_0 = \Phi^{-1} \left(\# \left(i \in \{1, 2, \dots, B\} : \hat{\rho}^*(i) < \hat{\rho}_s(\mathbf{x}, \mathbf{y}) \right) / B \right),$$

where Φ is the standard normal cumulative distribution function;

7 compute the **ORDERS OF PERCENTILES** as

$$\alpha_1 = \Phi \left(\hat{z}_0 + \frac{\hat{z}_0 + z^{(\alpha/2)}}{1 - \hat{a}(\hat{z}_0 + z^{(\alpha/2)})} \right),$$

$$\alpha_2 = \Phi \left(\hat{z}_0 + \frac{\hat{z}_0 + z^{(1-\alpha/2)}}{1 - \hat{a}(\hat{z}_0 + z^{(1-\alpha/2)})} \right),$$

where $z^{(\alpha/2)}$ and $z^{(1-\alpha/2)}$ are the $100 \cdot \alpha/2$ -th and the $100 \cdot (1 - \alpha/2)$ -th percentile points of the standard normal distribution, respectively.

TABLE 3 Pseudo-code of the bootstrap procedure used to carry out the test for the equality of two Spearman Matrices.

Algorithm 3: Bootstrap based test for the equality of two Spearman Matrices.

Input: Two multivariate Functional dataset

$$\mathbf{X} = \begin{bmatrix} x_{1,1}(t) & x_{1,2}(t) & \dots & x_{1,h}(t) \\ x_{2,1}(t) & x_{2,2}(t) & \dots & x_{2,h}(t) \\ \dots & \dots & \dots & \dots \\ x_{n_x,1}(t) & x_{n_x,2}(t) & \dots & x_{n_x,h}(t) \end{bmatrix}_{t \in T},$$

$$\mathbf{Y} = \begin{bmatrix} y_{1,1}(t) & y_{1,2}(t) & \dots & y_{1,h}(t) \\ y_{2,1}(t) & y_{2,2}(t) & \dots & y_{2,h}(t) \\ \dots & \dots & \dots & \dots \\ y_{n_y,1}(t) & y_{n_y,2}(t) & \dots & y_{n_y,h}(t) \end{bmatrix}_{t \in T},$$

from \mathbf{X}_t and \mathbf{Y}_t , respectively.

1 **for** $i \in 1, \dots, B$ **do**

2 obtain two **BOOTSTRAP DATASET** of multivariate functional data $\mathbf{X}_0^*, \mathbf{Y}_0^*$ by resampling from the original datasets \mathbf{X}, \mathbf{Y} under the null hypothesis;

3 compute the **BOOTSTRAP REPLICATION**

$$\Phi_0^*(i) = \|\widehat{SM}(\mathbf{X}_0^*) - \widehat{SM}(\mathbf{Y}_0^*)\|$$

4 estimate the **P-VALUE** of the test as

$$p = \#\left(i \in \{1, 2, \dots, B\} : \Phi_0^*(i) \geq \Phi(\mathbf{X}, \mathbf{Y})\right) / B.$$

4 | CASE STUDY: DETECTION OF ABERRATIONS IN DEPENDENCY PATTERNS AMONG HEALTHY AND UNHEALTHY PEOPLE USING ECG SIGNALS.

In this Section, we apply the techniques previously described to a real case study. The aim is to compare the Spearman Matrix arising from the h -variate ($h = 8$) electrocardiographic signals (ECGs hereafter) of a population of healthy people with the one arising from signals of people affected by Left Bundle Branch Block (LBBB hereafter), a kind of Acute Myocardial Infarction (see ?? for details about data and precise description of the pathology). Our goal is to investigate if the pattern of dependency between the components of the multivariate signals associated to each patient presents remarkable differences (aberration) in the two cases, due to the presence of the disease.

4.1 | Dataset description

Each statistical unit (patient) is characterized by the 8-variate functional datum of his/her electrocardiogram, which describes his/her heart dynamics on the eight leads I, II, V1, V2, V3, V4, V5 and V6, respectively. The data are from PROMETEO (PROgetto sull' area Milanese Elettrocardiogrammi Teletrasferiti dall'Extra Ospedaliero) database. PROMETEO project has been started in 2008 with the aim of spreading the intensive use of ECGs as pre-hospital diagnostic tool. The project is also a way of constructing a new database of ECGs with features never recorded before in any other data collection on heart diseases. See [Ieva et al. \(2013\)](#), [Tarabelloni et al. \(2015\)](#), [Ieva and Paganoni \(2016\)](#), [Ieva and Paganoni \(2017\)](#) for further details on the dataset and its use for statistical applications. The `roahd` package contains a toy-dataset reproducing a synthetic dataset inspired to this project, that is detailed in [Ieva et al. \(2018\)](#).

Each file contained in the PROMETEO database is associated to three sub-files, called *Details*, *Rhythm* and *Median*. For the aims of the present analysis, only the last one is necessary. The *Median* file depicts a reference beat lasting 1.2 seconds on a grid of 1200 points. It then provides 8 curves (one for each ECG lead) for each patient, representing patient's "median" beat for that lead. This representative heartbeat is a trace of a single cardiac cycle (heartbeat), i.e., of a P wave, a QRS complex, a T wave, and a U wave (see [Ieva et al. \(2013\)](#) for further details on ECG signals and their preprocessing).

Actually PROMETEO database contains 6,734 curves; among these, 1,633 are healthy (i.e., not affected by cardiovascular diseases detectable through the ECG), whereas 5,101 are affected by different heart diseases. As we said before, we will focus on Left Bundle Branch Block (LBBB). In the PROMETEO dataset, 314 people are affected by this pathology. After suitable preprocessing and robustification (see [Ieva and Paganoni \(2017\)](#) for more details) of the dataset, the sample available for the analyses is composed by 1,564 Physiological curves and 205 LBBB curves, discretized on a uniformly time grid T of 1024 points. Each patient is represented by his/her discretized multivariate signal, i.e., for $i = 1, \dots, n$, $\Phi_i(t) : T \subset \mathbb{R} \rightarrow \mathbb{R}^8$. All the curves of the available sample are registered and denoised according to the procedure described in [Ieva et al. \(2013\)](#).

To fix the notation, we assume that the ECG signals of physiological and pathological patients are realizations of two different multivariate stochastic processes, $\mathbf{X}_t = (X_t^1, X_t^2, \dots, X_t^8)$ and $\mathbf{Y}_t = (Y_t^1, Y_t^2, \dots, Y_t^8)$, respectively. Without loss of generality, in order to ease computations, we selected two balanced (results with the unbalanced case are the same) subsets of multivariate functional data: the first is denoted with \mathbf{X} and collects $n_x = 200$ randomly chosen ECG signals from the population of the physiological (healthy) patients. In other words, \mathbf{X} is a dataset composed by 200×8 discretized functions, where the i -th row contains the multivariate curve (ECG) associated to the i -th selected patient. The second functional dataset is denoted with \mathbf{Y} and contains the multivariate curves of $n_y = 200$ randomly chosen patients affected by LBBB. Figures 1 and 2 show the ECG signals selected in the datasets \mathbf{X} and \mathbf{Y} , respectively.

4.2 | Inference on the Spearman matrices of healthy vs LBBB patients

As we said before, we aim at studying the pattern of dependence among leads in the two populations of patients and pointing out possibly significant differences. This aim is supported by the following argument: it is likely, clinically speaking, that the presence of the disease might affect the way the leads depend on each other. In fact, the LBBB patients have a region of the heart that is damaged, and this modifies the heart dynamics. So, we believe that the relation of dependence among leads may change due to the presence of the disease. In what follows, we will apply techniques presented along the paper to the real case study described in the previous Section, in order to assess the statement above.

Tables 4 and 5 show the Spearman matrices for physiological ($\widehat{SM}(X)$) and pathological ($\widehat{SM}(Y)$) ECGs, respectively. The entries coloured in yellow represent the NON significant components of the pattern and indicate which pairs of leads can be assumed as uncorrelated according to the degree of dependency measured by the Spearman index. Their detection is performed observing the confidence intervals contained in the matrices $\widehat{SM}(X)_{0.95}$ and $\widehat{SM}(Y)_{0.95}$ (reported in Tables 6 and 7, respectively). We remind that, according to the procedure described in 3.3, if a confidence interval among a pair of components contains zero, the hypothesis of independence between the corresponding pair of leads is not rejected. In such a case, the component of the Spearman Matrix is coloured in order to highlight a non significant dependence. We decide to highlight the uncorrelated pairs of leads instead of the dependent ones in order to point out, in a easier way, the dissimilarities between the patterns, if any.

	I	II	V1	V2	V3	V4	V5	V6
I	1	0.357	-0.039	0.193	0.166	0.185	0.226	0.264
II		1	0.045	0.212	0.457	0.554	0.589	0.630
V1			1	0.713	0.451	0.304	0.255	0.173
V2				1	0.709	0.571	0.501	0.361
V3					1	0.879	0.761	0.575
V4						1	0.905	0.710
V5							1	0.843
V6								1

TABLE 4 Spearman Matrix for the population of the physiological signals. The non significant components (highlighted in yellow) are detected according to the confidence intervals of Table 6.

The two matrices provide an effective insight on the way the leads of the ECG signals depend one on each other. It can be noticed that the upper diagonals of the matrices almost always present high and significant values for the Spearman correlation coefficient. This means that, in both cases, the dynamics of the heart on a lead is strictly related to the dynamics on the following one. However, we notice remarkable differences in the two matrices. For instance, the pattern of dependence of physiological signals is more “connected”, whereas the one of LBBBs is more “sparse”, due to the presence of several pairs of uncorrelated leads. Moreover, it seems that the V2 lead dynamic is particularly affected by the presence of the disease. In fact, in healthy patients, it is significantly dependent on all the other leads, but the same does not hold in the pathological patients, where it is correlated only with 3 other leads.

What we observe can be interpreted in terms of heart dynamics in the following way: in physiological patients, the

	I	II	V1	V2	V3	V4	V5	V6
I	1	0.451	-0.378	-0.043	-0.037	0.337	0.612	0.659
II		1	-0.077	0.053	0.182	0.459	0.589	0.569
V1			1	0.756	0.559	0.136	-0.210	-0.366
V2				1	0.723	0.368	0.018	-0.144
V3					1	0.682	0.220	-0.058
V4						1	0.715	0.438
V5							1	0.844
V6								1

TABLE 5 Spearman Matrix for the population of the LBBB signals. The non significant components (highlighted in yellow) are detected according to the confidence intervals of Table 7.

dynamic of the heart is more regular and expresses a coordinated behaviour which is reflected on the ECG components dynamic, whereas it becomes more chaotic and characterized by disjointed behaviours of the parts when the pathology is present. Another difference that can be noticed comparing the two matrices is that, in the case of physiological signals, the entries that are significantly different from zero are positive, indicating that the leads tend to be monotone increasing functions of each other. The same does not happen for the LBBB signals, where the entries associated to the pairs V1-V5 and V1-V6 are negative. Hence, it seems that the disease is able to change the natural relation of dependence among some leads of the ECG.

	I	II	V1	V2	V3	V4	V5	V6
I	1	(0.227, 0.470)	(-0.179, 0.089)	(0.071, 0.311)	(0.010, 0.292)	(0.054, 0.312)	(0.100, 0.352)	(0.140, 0.389)
II		1	(-0.097, 0.185)	(0.050, 0.336)	(0.331, 0.566)	(0.429, 0.648)	(0.476, 0.678)	(0.527, 0.716)
V1			1	(0.597, 0.773)	(0.348, 0.563)	(0.163, 0.409)	(0.125, 0.378)	(0.037, 0.300)
V2				1	(0.633, 0.768)	(0.479, 0.657)	(0.392, 0.590)	(0.239, 0.484)
V3					1	(0.842, 0.906)	(0.694, 0.808)	(0.458, 0.658)
V4						1	(0.871, 0.927)	(0.595, 0.784)
V5							1	(0.771, 0.892)
V6								1

TABLE 6 Matrix of confidence intervals of coverage probability 0.95 for the components of the Spearman Matrix associated to the population of the physiological signals. Each interval is computed using $B = 1000$ bootstrap iterations. The intervals containing zero are highlighted in yellow.

The differences highlighted above lead us to suppose that the patterns of dependence of the two populations of signals are different. A quantitative confirmation of this conjecture is given performing the bootstrap test for the equality of two Spearman matrices introduced in Section 3.5.

Let's consider the distance among matrices induced by the *one norm* (results does not change considering any other type of distance). Figure 3 reports the histogram of $B = 1000$ bootstrap replications of statistics Φ under H_0 . The dashed line denotes the observed value $\Phi(\mathbf{X}, \mathbf{Y})$. As you can see, the value obtained for the statistical test indicates that the observed value is not likely under the null hypothesis (p -value $< 2e-16$). Therefore, the test gives strong evidence to

	I	II	V1	V2	V3	V4	V5	V6
I	1	(0.294, 0.557)	(-0.494, -0.242)	(-0.188, 0.106)	(-0.181, 0.096)	(0.211, 0.446)	(0.505, 0.694)	(0.559, 0.731)
II		1	(-0.226, 0.080)	(-0.121, 0.194)	(0.022, 0.322)	(0.340, 0.568)	(0.474, 0.670)	(0.452, 0.667)
V1			1	(0.674, 0.814)	(0.455, 0.644)	(-0.012, 0.272)	(-0.360, -0.054)	(-0.487, -0.224)
V2				1	(0.646, 0.791)	(0.216, 0.495)	(-0.137, 0.197)	(-0.300, 0.009)
V3					1	(0.546, 0.761)	(0.043, 0.373)	(-0.192, 0.086)
V4						1	(0.635, 0.787)	(0.319, 0.545)
V5							1	(0.783, 0.889)
V6								1

TABLE 7 Matrix of confidence intervals of coverage probability 0.95 for the components of the Spearman Matrix associated to the population of the pathological signals. Each interval is computed using $B = 1000$ bootstrap iterations. The intervals containing zero are highlighted in yellow.

reject H_0 and to state that the Spearman matrices of physiological and pathological signals are different.

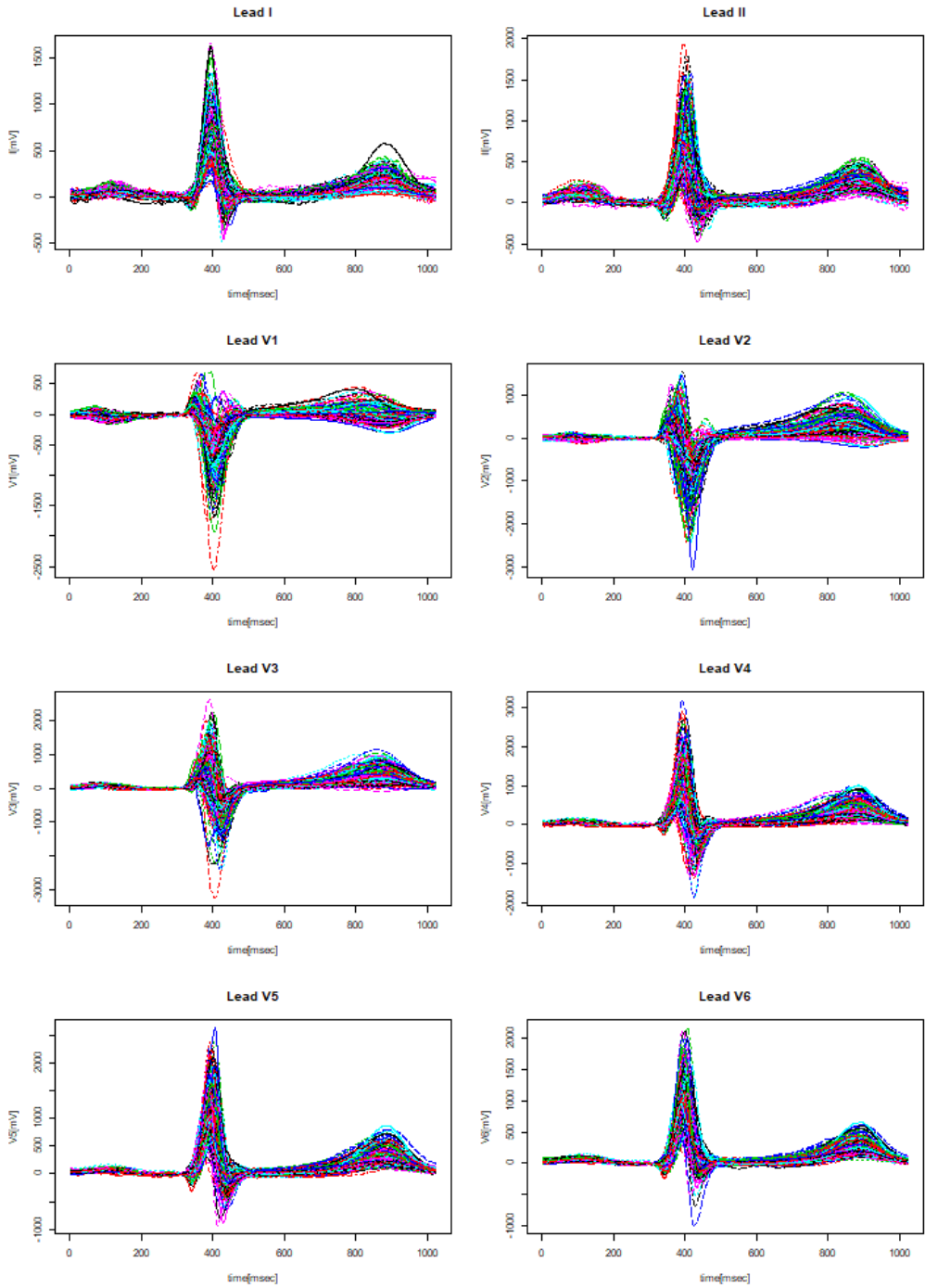


FIGURE 1 Registered and denoised ECG signals of the $n_x = 200$ physiological patients used for the analysis.

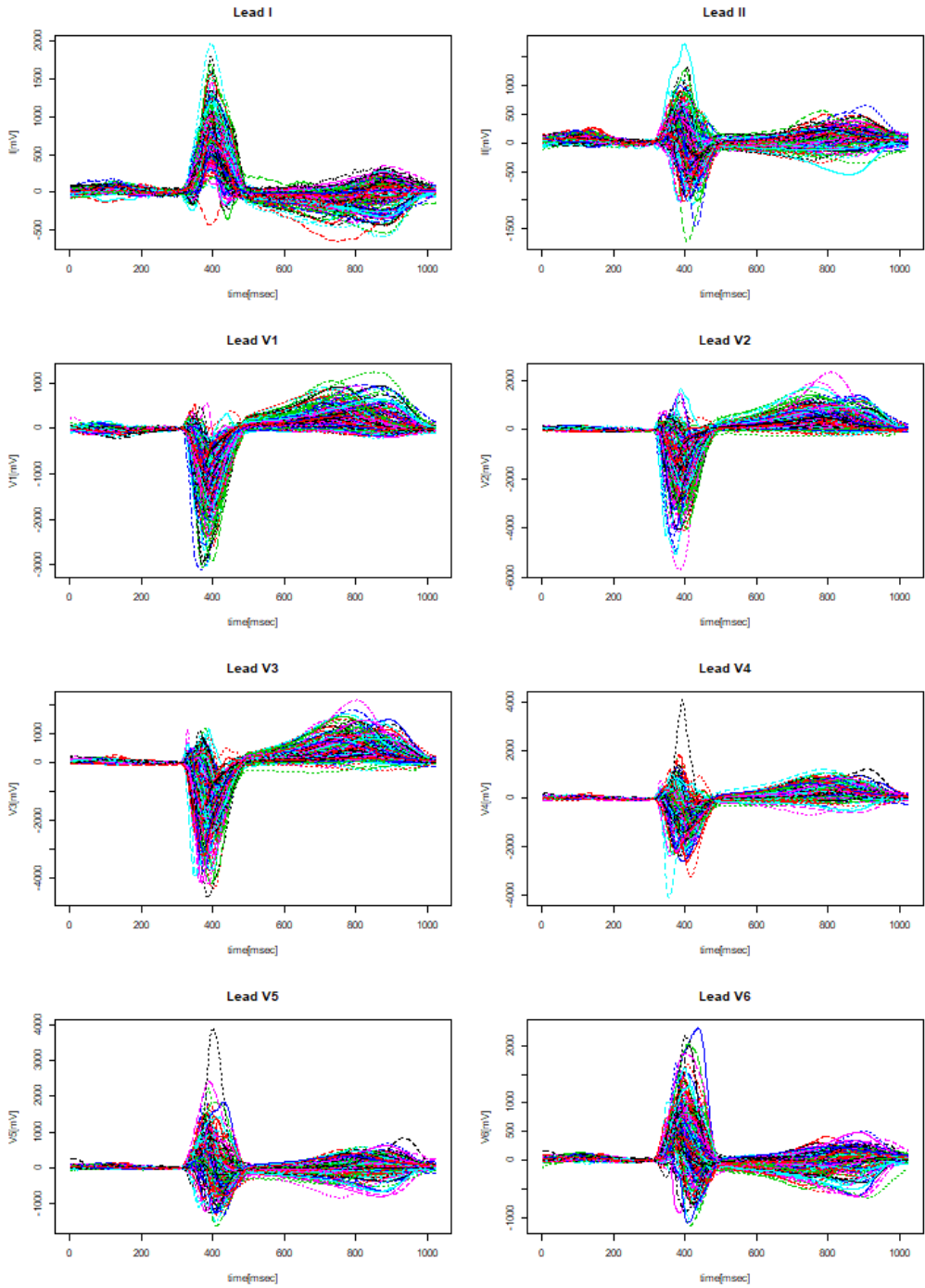


FIGURE 2 Registered and denoised ECG signals of the $n_y = 200$ LBBB patients used for the analysis.

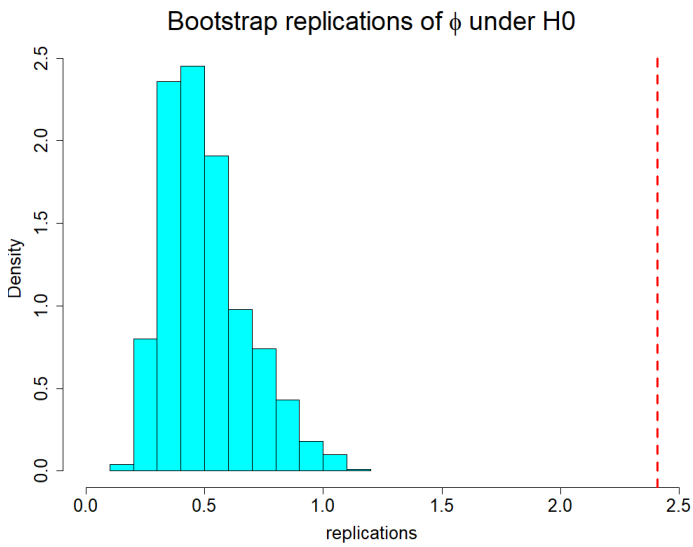


FIGURE 3 Histogram of $B = 1000$ bootstrap replications of Φ under H_0 computed using the distance induced by the one norm. The dashed line is drawn at the observed values $\Phi(\mathbf{X}, \mathbf{Y}) = 2.41$.

5 | DISCUSSION AND CONCLUSIONS

The investigation of the dependence among curves is relatively a new issue in statistics. This is mainly due to the late development of (multivariate) functional data analysis with respect to multivariate analysis as well as to the difficulty in summarizing dependence and other indexes in the infinite dimensional context. Indeed, treating the problem of estimating dependency in (multivariate) functional setting is not a straightforward task. On the other hand, it is more and more often the case that disciplines like medicine, finance, quality control, and many others bring to statistical stage complex and high dimensional data (e.g. signals) which require suitable techniques to be handled and used for inference and prediction purposes.

For all these reasons, in this paper we considered the definition of the Spearman index for function introduced by Valencia et al. (2016) as a starting point to set a suitable bootstrap based inferential setting for assessing dependency among families of (multivariate) curves. The main contribution of the work is twofold: firstly, we provided and handleable and intuitive set of instruments for assessing dependency among families of (multivariate) functional data; secondly, we formalized a computationally feasible and effective framework for performing inference on it.

Further developments of the work may take both the theoretical and applied setting. They may regard, among others: i) the deeper study of the relationship among Spearman index ρ_s and the correlation ρ overimposed in the simulation study among functions; ii) the joint inference for more than two families of curves; iii) the validation of results on different cardiac pathologies or disease contexts, like the analysis of brain signals in patients where connections among different parts of the brain have been damaged by a disease or compromised by a surgical intervention.

ACKNOWLEDGEMENTS

The authors wish to thank Nicholas Tarabelloni for helping with `roabd` coding of the present functions.

APPENDIX A: ON THE NOTION OF BOOTSTRAP CONFIDENCE INTERVALS

In this Section, the notion of bootstrap replication of a statistic is exploited to compute confidence interval for a given unknown parameter of interest. Suppose that the data $\mathbf{x} = (x_1, x_2, \dots, x_n)$ are obtained by random sampling from an univariate unknown distribution F . Let $\theta = t(F)$ the parameter on which we want to make inference on and suppose that $\hat{\theta}$ is the estimate of θ based on \mathbf{x} , say $\hat{\theta} = T_n(\mathbf{x})$. A possible way for defining a confidence interval for θ is to use the so called *percentile interval*, based on the percentiles of the bootstrap distribution of the statistic T_n . Let \mathbf{x}^* be a bootstrap sample drawn from data and consider the bootstrap replication of $\hat{\theta}$, say $\hat{\theta}^* = T_n(\mathbf{x}^*)$. Let \hat{Q} be the cumulative distribution function of $\hat{\theta}^*$. The $1 - \alpha$ *percentile interval* is defined by the $\alpha/2$ and $1 - \alpha/2$ percentiles of \hat{Q} :

$$(\hat{\theta}_{lo}, \hat{\theta}_{up}) = (\hat{Q}^{-1}(\alpha/2), \hat{Q}^{-1}(1 - \alpha/2)). \quad (5.1)$$

Since by the definition $\hat{Q}^{-1}(\alpha/2) = \hat{\theta}^{*(\alpha/2)}$, the $100 \cdot \alpha/2$ th percentile of the bootstrap distribution, we can also write the percentile interval as

$$(\hat{\theta}_{lo}, \hat{\theta}_{up}) = (\hat{\theta}^{*(\alpha/2)}, \hat{\theta}^{*(1-\alpha/2)}). \quad (5.2)$$

Expressions (5.1) and (5.2) refer to the ideal bootstrap situation in which the number of bootstrap replications is infinite.

In practice, we must use some finite number B of replications. Hence, we can generate B independent bootstrap datasets $\mathbf{x}_1^*, \mathbf{x}_2^*, \dots, \mathbf{x}_B^*$ and compute the bootstrap replication $\hat{\theta}^*(i) = T_n(\mathbf{x}_i^*)$, $i = 1, 2, \dots, B$. Let $\hat{\theta}_B^{*(\alpha/2)}$ be the $100 \cdot \alpha/2$ th empirical percentile of the $\hat{\theta}^*(i)$ values, that is, the $B \cdot \alpha/2$ th value in the ordered list of the B replications of $\hat{\theta}^*$. Hence, if $B = 2000$ and $\alpha = 0.1$, $\hat{\theta}_B^{*(\alpha)}$ is the 100th ordered value of the replications. Likewise, let $\hat{\theta}_B^{*(1-\alpha/2)}$ be the $100 \cdot (1 - \alpha/2)$ th empirical percentile. If $B \cdot \alpha/2$ is not an integer, the following convention can be used. Assuming $\alpha/2 \leq 0.5$, let $k = \lfloor (B+1)\alpha/2 \rfloor$, the largest integer $\leq (B+1)\alpha/2$. Then the $100 \cdot \alpha/2$ th and the $100 \cdot (1 - \alpha/2)$ th empirical percentiles are defined, respectively, as the k th and $(B+1-k)$ th values in the ordered list of the B replications. Given these notions, the approximate $1 - \alpha$ percentile interval is

$$(\hat{\theta}_{lo}, \hat{\theta}_{up}) \approx (\hat{\theta}_B^{*(\alpha/2)}, \hat{\theta}_B^{*(1-\alpha/2)}). \quad (5.3)$$

Despite the fact that they are very easy to compute, these intervals present some critical issues, as explained in [Efron and Tibshirani \(1993\)](#). For instance, they have bad coverage performances, in the sense that the level $1 - \alpha$ is an overestimate of the real coverage probability. This is a consequence of the fact that the percentile intervals do not take in account the possible bias associated to the point estimate $\hat{\theta}$. Moreover, they implicitly assume that the standard error of the estimate does not depend on the value of the unknown parameter θ , but in real applications this may happen.

The latter argument induces us to consider an improved version of the percentile method called BC_a (*bias-corrected and accelerated*). The BC_a intervals are a substantial improvement over the percentile method in both theory and practice, since they are more accurate in terms of coverage probability. We presented the $1 - \alpha$ percentile interval as

$$\text{percentile method : } (\hat{\theta}_{lo}, \hat{\theta}_{up}) = (\hat{\theta}^{*(\alpha/2)}, \hat{\theta}^{*(1-\alpha/2)}). \quad (5.4)$$

The BC_a interval endpoints are also given by the percentiles of the bootstrap distribution, but not necessarily the same ones as in (5.4). In fact, the percentiles used in the new approach depend on two numbers \hat{a} and \hat{z}_0 , called the *acceleration* and *bias-correction*, respectively. We give first the definition of the BC_a interval endpoints and then we describe how \hat{a} and \hat{z}_0 are obtained.

The BC_a interval of intended coverage probability $1 - \alpha$, is defined by

$$BC_a : (\hat{\theta}_{lo}, \hat{\theta}_{up}) = (\hat{\theta}^{*(\alpha_1)}, \hat{\theta}^{*(\alpha_2)}), \quad (5.5)$$

where

$$\begin{aligned} \alpha_1 &= \Phi\left(\hat{z}_0 + \frac{\hat{z}_0 + z^{(\alpha/2)}}{1 - \hat{a}(\hat{z}_0 + z^{(\alpha/2)})}\right), \\ \alpha_2 &= \Phi\left(\hat{z}_0 + \frac{\hat{z}_0 + z^{(1-\alpha/2)}}{1 - \hat{a}(\hat{z}_0 + z^{(1-\alpha/2)})}\right). \end{aligned} \quad (5.6)$$

Here Φ is the standard normal cumulative distribution function and $z^{(\alpha)}$ and $z^{(1-\alpha/2)}$ are the $100 \cdot \alpha/2$ th and the $100 \cdot (1 - \alpha/2)$ th percentile points of the standard normal distribution, respectively. Formula (5.6) looks complicated, but it is easy to compute. Notice that if \hat{a} and \hat{z}_0 equal zero, then

$$\alpha_1 = \Phi(z^{(\alpha/2)}) = \alpha/2 \quad \text{and} \quad \alpha_2 = \Phi(z^{(1-\alpha/2)}) = 1 - \alpha/2, \quad (5.7)$$

so that the BC_a interval (5.5) is the same as the percentile interval (5.4). Non-zero values of \hat{a} and \hat{z}_0 change the percentiles used for the BC_a endpoints, correcting the deficiencies of the percentile method (see Efron and Tibshirani (1993) for further details).

The value of bias-correction \hat{z}_0 is obtained directly from the proportion of bootstrap replications less than the original estimate $\hat{\theta}$,

$$\hat{z}_0 = \Phi^{-1} \left(\# \left(i \in \{1, 2, \dots, B\} : \hat{\theta}^*(i) < \hat{\theta} \right) / B \right), \quad (5.8)$$

where Φ^{-1} indicates the inverse function of a standard normal cumulative distribution function. Roughly speaking, \hat{z}_0 measures the median bias of $\hat{\theta}^*$, say the discrepancy between the median of $\hat{\theta}^*$ and $\hat{\theta}$, in normal units. This represents also a measure of the median bias of the estimate $\hat{\theta}$. Of course, we obtain $\hat{z}_0 = 0$ if exactly half of the $\hat{\theta}^*(i)$ values are less than or equal to $\hat{\theta}$. There are various ways to compute the acceleration \hat{a} . The easiest to explain is given in terms of the *jackknife values* of the statistic $\hat{\theta} = T_n(\mathbf{x})$. Let $\mathbf{x}_{(i)}$ be the original sample with the i th point x_i deleted. Moreover, let $\hat{\theta}_{(i)} = T_n(\mathbf{x}_{(i)})$ and define $\hat{\theta}_{(\cdot)} = \sum_{i=1}^n \hat{\theta}_{(i)} / n$. A simple expression for the acceleration is

$$\hat{a} = \frac{\sum_{i=1}^n (\hat{\theta}_{(\cdot)} - \hat{\theta}_{(i)})^3}{6 \{ \sum_{i=1}^n (\hat{\theta}_{(\cdot)} - \hat{\theta}_{(i)})^2 \}^{3/2}}. \quad (5.9)$$

The name acceleration is due to the fact that it refers to the rate of change of the standard error of $\hat{\theta}$ with respect to the true parameter value θ , measured on a normalized scale. Therefore, through the acceleration, the interval takes in account also the possibility that the variability of the point estimate depends on the value of the unknown parameter. This adjustment improves the performance with respect to the percentile method. It is not all obvious why the formula (5.9) should provide an estimate of the acceleration of the standard error. Some discussions of this may be found in Efron (1987).

APPENDIX B: SIMULATION STUDY

In this Section we present some simulation studies aimed at testing the performance of the Spearman index and Matrix estimators introduced in Section 2 of the paper, when correlation among the components of multivariate curves exists/does not exist, is direct/inverse, respectively.

Without loss of generality, in the first part of the study, we consider bivariate functional datasets (Case 1, $h = 2$), sampled from a stochastic process (X_t, Y_t) . In this case, we investigate the dependence between the components of the generative process providing the point and interval estimates of the Spearman index and performing the independence test introduced in Subsection 3.3. Then we consider a multivariate functional dataset (Case 2, $h > 2$). In this case, we investigate the pattern of dependence between the components computing the point estimate of the Spearman Matrix and evaluating the significance of its entries using confidence intervals introduced in Section 3.4.

| Case 1: bivariate functional data

The first part of the study considers functional observations with $h = 2$ components, sampled from the reference model proposed in Ieva and Paganoni (2017). Let

$$(X_t, Y_t) = (\mu_X(t) + \mathbb{Z}_X(t), \mu_Y(t) + \mathbb{Z}_Y(t)), \quad (5.10)$$

be a bivariate gaussian process with means

$$\begin{aligned}\mu_X(t) &= \sin(2\pi t), \quad t \in I = [0, 1], \\ \mu_Y(t) &= \sin(4\pi t), \quad t \in I = [0, 1],\end{aligned}$$

and exponential Matérn covariance functions

$$\begin{aligned}\text{Cov}(\mathbb{Z}_X(t), \mathbb{Z}_X(s)) &= C_X(t, s) = \alpha_X \exp(\beta_X |s - t|), \\ \text{Cov}(\mathbb{Z}_Y(t), \mathbb{Z}_Y(s)) &= C_Y(t, s) = \alpha_Y \exp(\beta_Y |s - t|). \quad t, s \in I.\end{aligned}$$

In the following, we will always set $\alpha_X = 0.5$, $\alpha_Y = 0.7$, $\beta_X = \beta_Y = 0.4$ without loss of generality.

We introduce a dependence between the two components of the process assuming a correlation between $\mathbb{Z}_X(t)$ and $\mathbb{Z}_Y(t)$, say

$$\text{Corr}(\mathbb{Z}_X(t), \mathbb{Z}_Y(t)) = \rho, \quad \forall t \in I.$$

It is important to remark that the data generation procedure adopted above assumes a pointwise dependence between the curves. This kind of dependence is different from the one theoretically captured by the Spearman index. In fact, $\rho_s(X_t, Y_t)$ considers the direction of association between X_t and Y_t , namely their tendency to be perfect monotone (increasing or decreasing) function of each other. Therefore, it takes into account the possible dependence between the processes behaviours in the reference time interval and not only the pointwise correlation between their points, as the variance-covariance operator would do. Of course, the reciprocal behaviour of X_t and Y_t is influenced by the correlation ρ that we impose in the generating model, but the two concepts are not completely overlapped, since they are also influenced by the means that we choose for the processes, among others. For this reason, when we fix ρ , we do not fix $\rho_s(X_t, Y_t)$ and this means that a priori we cannot expect that the point estimate $\hat{\rho}_s$ of the Spearman index is also an estimate of ρ , even if they are of course related in some sense. In our simulation, ρ is used to vary the grade of dependence between the components, in order to obtain different scenarios for the evaluation of the performances of our tools.

In Figure 4 a sample of $n = 200$ bivariate curves from the stochastic process described above is presented, assuming uncorrelated components, i.e., $\rho = 0$.

Given this framework, we can sample functional datasets from the model (5.10) and then make inference on the Spearman index characterizing them. We simulate six samples, each of them composed by $n = 200$ bivariate curves, defined over an uniformly time grid of $d = 500$ points and characterized by a pointwise correlation ρ among components ranging in $\{0.01, 0.1, 0.3, 0.6, 0.9, 0.999\}$. For the bootstrap estimates, $B = 1000$ iterations are considered. The inference on ρ_s is performed providing:

- The value of the point estimate $\hat{\rho}_s$, computed using the Inferior Length grade (results does not change considering the Superior Length grade).
- The BC_α confidence interval for ρ_s of intended coverage probability $1 - \alpha = 0.95$.
- The result of the independence test presented in Subsection 3.3.

The results are summarized in Table 8.

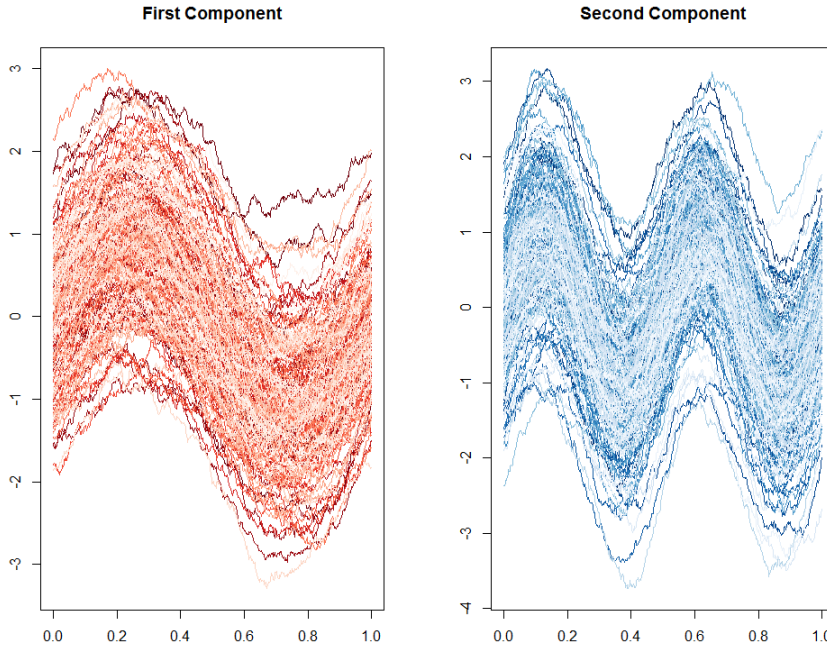


FIGURE 4 Sample of $n = 200$ bivariate curves with no correlations among components ($\rho = 0$).

ρ	$\hat{\rho}_s$	$CI_{0.95}(\rho_s)$		Result of the test
0.01	-0.045	-0.188	0.098	not reject
0.1	0.068	-0.065	0.212	not reject
0.3	0.393	0.248	0.505	reject
0.6	0.712	0.640	0.776	reject
0.9	0.885	0.845	0.910	reject
0.999	0.998	0.997	0.999	reject

TABLE 8 Inference on ρ_s using bivariate functional samples of $n = 200$ curves with pointwise correlation ranging from 0.01 to 0.999.

First of all, we notice that $\hat{\rho}_s$ seems able to capture the dependence between the components of the bivariate curves, if any. In fact, if we set a sufficiently large pointwise correlation, the point estimate is positive and significantly different from 0, where significantly means that the corresponding BC_a confidence interval does not contain 0. This result confirms the theoretical properties of the Spearman index discussed in Section ???. Consider now the case in which the pointwise correlation is small, say $\rho = 0.01$ and $\rho = 0.1$. In these cases the point estimator provides a value different from 0, but not far from it and actually not significant, since the corresponding confidence interval does contain 0.

Correspondingly, in the independence test the null hypothesis is rejected at a significance level $\alpha = 0.05$ when there is a strong pointwise correlation between the components of the bivariate curves. In other words, the presence of dependence is correctly kept by the test. On the other hand, when the pointwise correlation is weak, the test does not provide evidence for rejecting the hypothesis of independence.

From Table 8, it can be also noticed that the BC_a confidence intervals of coverage probability 0.95 always contain the value of pointwise correlation ρ , except for the case $\rho = 0.6$. As we discussed above, this is due to the fact that ρ and $\rho_s(X_t, Y_t)$ are not the same thing. However, since the two concepts are linked, confidence intervals for ρ_s might be considered, in the most part of cases, as good interval estimators of the pointwise correlation.

To complete our analysis, we perform the same inference considering also functional datasets with negative pointwise correlations among components. Again, we consider six samples of $n = 200$ bivariate curves defined over an uniformly time grid of $d = 500$ points, with ρ ranging in $\{-0.999, -0.9, -0.6, -0.3, -0.1, -0.01\}$. For the computation of the interval estimates, we fix $B = 1000$. The results are summarized in Table 9.

ρ	$\hat{\rho}_s$	$CI_{0.95}(\rho_s)$		Result of the test
-0.999	-0.998	-0.999	-0.998	reject
-0.9	-0.874	-0.906	-0.831	reject
-0.6	-0.555	-0.643	-0.444	reject
-0.3	-0.211	-0.341	-0.082	reject
-0.1	-0.044	-0.173	0.093	not reject
-0.01	0.002	-0.138	0.140	not reject

TABLE 9 Inference on ρ_s using bivariate functional samples of $n = 200$ curves with pointwise correlation ranging from -0.999 to -0.01.

The results are satisfactory also in this case. The point estimates of the Spearman index are significant when a significantly high negative correlation is present, while they are not significant when the correlation is weak. So we can say that the Spearman index has good performance also in case of negative dependence between the components. Again, the independence test rejects the null hypothesis only when the correlations among the component is strong.

| Case 2: h -variate functional data

We now consider functional data generated by a multivariate stochastic process $\mathbf{X}_t = (X_t^1, X_t^2, \dots, X_t^h)$, with $h > 2$. In this case, the object of the inference is the pattern of dependence among the components of the process, captured by the Spearman Matrix $SM(\mathbf{X}_t)$. Without lack of generality, we focus on trivariate case, say $h = 3$.

Let's consider a trivariate gaussian process, generated by the following model:

$$(X_t^1, X_t^2, X_t^3) = (\mu_1(t) + Z_1(t), \mu_2(t) + Z_2(t), \mu_3(t) + Z_3(t)),$$

with means

$$\begin{aligned}\mu_1(t) &= \sin(2\pi t), & t \in I = [0, 1], \\ \mu_2(t) &= \sin(4\pi t), & t \in I = [0, 1], \\ \mu_3(t) &= \sin(6\pi t), & t \in I = [0, 1],\end{aligned}$$

and exponential Matérn covariance functions

$$\begin{aligned}\text{Cov}(\mathbb{Z}_1(t), \mathbb{Z}_1(s)) &= C_1(t, s) = \alpha_1 \exp(\beta_1 |s - t|), \\ \text{Cov}(\mathbb{Z}_2(t), \mathbb{Z}_2(s)) &= C_2(t, s) = \alpha_2 \exp(\beta_2 |s - t|), \\ \text{Cov}(\mathbb{Z}_3(t), \mathbb{Z}_3(s)) &= C_3(t, s) = \alpha_3 \exp(\beta_3 |s - t|) \quad t, s \in I.\end{aligned}$$

In the following, we set $\alpha_1 = 0.5$, $\alpha_2 = 0.7$, $\alpha_3 = 0.8$, $\beta_1 = \beta_2 = \beta_3 = 0.4$ without loss of generality. We introduce a dependence between the components of the trivariate process assuming a correlation structure between $\mathbb{Z}_1(t)$, $\mathbb{Z}_2(t)$ and $\mathbb{Z}_3(t)$, say

$$\text{Corr}(\mathbb{Z}_1(t), \mathbb{Z}_2(t), \mathbb{Z}_3(t)) = \begin{bmatrix} 1 & \rho_{12} & \rho_{13} \\ & 1 & \rho_{23} \\ & & 1 \end{bmatrix}, \quad \forall t \in I.$$

Again, the dependence imposed by the pointwise correlation ρ_{ij} is different from the dependence captured by the ij component of the Spearman Matrix, according to the argument proposed in the previous paragraph. Therefore, a priori we cannot expect the sample estimate $\widehat{SM}(\mathbf{X})$ to be a point estimate of the matrix $\text{Corr}(\mathbb{Z}_1(t), \mathbb{Z}_2(t), \mathbb{Z}_3(t))$, but it is a reasonable proxy.

Given this framework, we carry out the inference. We simulate from the model $n = 200$ trivariate curves defined over a uniformly time grid of $d = 500$ points. The correlation structure used is

$$\text{Corr}(\mathbb{Z}_1(t), \mathbb{Z}_2(t), \mathbb{Z}_3(t)) = \begin{bmatrix} 1 & 0.9 & -0.3 \\ & 1 & 0.01 \\ & & 1 \end{bmatrix}, \quad \forall t \in I. \quad (5.11)$$

Basically, we are assuming a trivariate process with an high and positive correlation among the first and the second component, a very weak and positive correlation among the second and the third one and a weak and negative correlation among the first and the third one. For this instance, the point estimate of the Spearman Matrix is

$$\widehat{SM}(\mathbf{X}) = \begin{bmatrix} 1 & 0.895 & -0.350 \\ & 1 & -0.038 \\ & & 1 \end{bmatrix},$$

and the corresponding matrix of the BC_a confidence intervals with 0.95 coverage probability ($B=1000$) is given by

$$\widehat{SM}(\mathbf{X})_{0,95} = \begin{bmatrix} 1 & (0.857, 0.922) & (-0.471, -0.231) \\ & 1 & (-0.170, 0.086) \\ & & 1 \end{bmatrix}. \quad (5.12)$$

We can notice that $\widehat{SM}(\mathbf{X})$ provides a good representation of the grade of dependence between the components of the generative process. In fact, it indicates a large positive dependence between the first and the second component, a negative dependence between first and the third one and a very weak dependence between the second and the third one, coherently with the correlation structure defined in (5.11).

If we want to simplify the pattern of dependence, we can perform the disjointed tests

- $H_0: \rho_s(X_t^i, X_t^j) = 0$,
- $H_1: \rho_s(X_t^i, X_t^j) \neq 0$.

for $i = 1, 2, j = i + 1, \dots, 3$. From (5.12), we notice that only the confidence interval for $\rho_s(X_t^2, X_t^3)$ contains zero, indicating that the dependence captured by corresponding component of $\widehat{SM}(\mathbf{X})$ is not significant.

In general, we may say that the simulations carried out in this Section testify for good performances of the inferential tools proposed into the paper in properly capturing and describing the dependency among (multivariate) families of curves.

REFERENCES

- Dubin, J. A. and Muller, H. G. (2005) Dynamical correlation for multivariate longitudinal data. *Journal of the American Statistical Association*, 872–881.
- Efron, B. (1987) Better bootstrap confidence intervals. *Journal of the American Statistical Association*, 82, 171–185. URL: <https://www.tandfonline.com/doi/abs/10.1080/01621459.1987.10478410>.
- Efron, B. and Tibshirani, R. (1993) *An introduction to the Bootstrap*. Monographs on Statistics and Applied Probability. Chapman & Hall/CRC.
- Ferraty, F. and Vieu, P. (2006) *Nonparametric Functional Data Analysis: Theory and Practice*. Springer Series in Statistics. Springer-Verlag New York.
- Hauke, J. and Kossowski, T. (2011) Comparison of values of pearson's and spearman's correlation coefficients on the same sets of data. *Quaestiones Geographicae*, 2, 87–93.
- He, G., Muller, H. and Wang, J. (2000) Extending correlation and regression from multivariate to functional data. *Asymptotics in Statistics and Probability*, 197–201.
- (2004) Methods of canonical analysis for functional data. *Journal of Statistical Planning and Inference*, 141–159.
- Ieva, F. and Paganoni, A. (2016) Risk prediction for myocardial infarction via generalized functional regression models. *Statistical Methods in Medical Research*, 25, 1648–1660.
- (2017) A taxonomy of outlier detection methods for robust classification in multivariate functional data. *Statistical Papers*. Doi: 10.1007/s00362-017-0953-1.

- Ieva, F., Paganoni, A., Pigoli, D. and Vitelli, V. (2013) Multivariate functional clustering for the analysis of ecg curves morphology. *Journal of the Royal Statistical Society - Series C*, **62**, 401–418.
- Ieva, F., Paganoni, A., Romo, J. and Tarabelloni, N. (2018) roahd package: Robust analysis of high dimensional data. *Tech. rep.*, Department of Mathematics, Politecnico di Milano. Submitted.
- Kokoszka, P. and Reimherr, M. (2017) *Introduction to Functional Data Analysis*. Chapman and Hall/CRC.
- Leurgans, S., Moyeed, R. and Silverman, B. (1993) Canonical correlation analysis when data are curves. *Journal of the Royal Society - Series B*, 725–740.
- Li, R. and Chow, M. (2005) Evaluation of reproducibility for paired functional data. *Journal of Multivariate Analysis*, 81–101.
- Martin-Barragan, M., Lillo, R. and Romo, J. (2016) Functional boxplots based on epigraphs and hypographs. *Journal of Applied Statistics*, **43**, 1088–1103.
- Opgen-Rhein, R. and Strimmer, K. (2006) Inferring gene dependency networks from genomic longitudinal data: a functional data approach. *REVSTAT Statistical Journal*, 53–65.
- Ramsay, J. and Silverman, B. (2005) *Functional Data Analysis*. 0172-7397. Springer-Verlag New York.
- Spearman, C. (1904) The proof and measurement of association between two things. *American Journal of Psychology*, 72–101.
- Tarabelloni, N., Arribas-Gil, A., Ieva, F., Paganoni, A. and Romo, J. (2018) *roahd - RObust Analysis of High Dimensional Data*. URL: <https://cran.r-project.org/web/packages/roahd/roahd.pdf>.
- Tarabelloni, N., Ieva, F., Paganoni, A. and Biasi, R. (2015) Use of depth measure for multivariate functional data in disease prediction: an application to electrocardiograph signals. *International Journal of Biostatistics*, **11**, 189–201.
- Team, R. C. (2017) R: A language and environment for statistical computing. URL: <https://www.R-project.org/>.
- Valencia, D. (2014) *Dependence for functional data*. Ph.D. thesis, Department of Statistics, UC3M - University Carlos III of Madrid, Spain.
- Valencia, D., Lillo, R. and J., R. (2012) Functional kendall's tau. In *Joint Statistical Meetings (ASA)*. San Diego. URL: <https://www.dropbox.com/s/wezt3d6ofp7hsg4/ASA2012.pdf>.
- Valencia, D., Lillo, R. and Romo, J. (2016) Dependence for functions: Spearman coefficient. *Tech. rep.*, Department of Statistics, UC3M - University Carlos III of Madrid, Spain. Submitted.
- Xu, W., Hung, Y. and Zou, Y. (2010) Comparison of spearmans rho and kendalls tau in normal and contaminated normal models. *Tech. rep.* ArXiv:1011.2009.

MOX Technical Reports, last issues

Dipartimento di Matematica
Politecnico di Milano, Via Bonardi 9 - 20133 Milano (Italy)

- 29/2018** Manzoni, A; Bonomi, D.; Quarteroni, A.
Reduced order modeling for cardiac electrophysiology and mechanics: new methodologies, challenges & perspectives
- 28/2018** Gerbi, A.; Dede', L.; Quarteroni, A.
Segregated algorithms for the numerical simulation of cardiac electromechanics in the left human ventricle
- 25/2018** Chave, F.; Di Pietro, D.A.; Formaggia, L.
A Hybrid High-Order method for passive transport in fractured porous media
- 26/2018** Vergara, C.; Zonca, S.
Extended Finite Elements method for fluid-structure interaction with an immersed thick non-linear structure
- 27/2018** Antonietti, P.F.; Verani, M.; Vergara, C.; Zonca, S.
Numerical solution of fluid-structure interaction problems by means of a high order Discontinuous Galerkin method on polygonal grids
- 24/2018** Bassi, C.; Abbà, A.; Bonaventura, L.; Valdettaro, L.
Direct and Large Eddy Simulation of three-dimensional non-Boussinesq gravity currents with a high order DG method
- 22/2018** Pegolotti, L.; Dede', L.; Quarteroni, A.
Isogeometric Analysis of the electrophysiology in the human heart: numerical simulation of the bidomain equations on the atria
- 21/2018** Gervasio, P.; Dede', L.; Chanon, O.; Quarteroni, A.
Comparing Isogeometric Analysis and Spectral Element Methods: accuracy and spectral properties
- 23/2018** Benacchio, T.; Bonaventura, L.
A seamless extension of DG methods for hyperbolic problems to unbounded domains
- 20/2018** Bassi, C. ; Abbà, A.; Bonaventura L.; Valdettaro, L.
A priori tests of a novel LES approach to compressible variable density turbulence